Satellitesimal formation in a circumplanetary disk and pebble accretion

*Yuhito Shibaike[1], Satoshi Okuzumi[1], Takanori Sasaki[2]

1.Department of Earth and Planetary Sciences, Tokyo Institute of Technology, 2.Department of Astronomy, Kyoto University

It has been recently suggested that planetesimals rapidly grow to the cores of gas giants by accreting a number of cm-sized solid particles called pebbles. We investigate how this pebble accretion mechanism affects satellite formation around gas giants. We construct a simple but comprehensive model that treats 1) the growth and radial transport of pebble-sized dust particles in a protoplanetary disk and in a circumplanetary disk around a gas giant, 2) the inflows of the gas and pebbles from protoplanetary to circumplanetary disks, and 3) pebble accretion by satellitesimals in a circumplanetary disk.
We found that most of pebbles flow into a circumplanetary disk not from the high-altitude of the disk but from the mid-plane against gas outflows. We also found that the growth processes of pebbles in a circumplanetary disk are divided into two much different ways; 1) satellitesimal formation by direct collisional growth of pebbles and subsequent satellite formation by direct collisional growth of the satellitesimals in a critical orbit, and 2) pebble accretion by large satellitesimals outside of the critical orbit. The critical orbit is moved by the conditions of the disk and pebbles. We introduce a parameter x, the ratio of the two mass fluxes of pebbles; flowing into the circumplanetary disk and drifted from the outer region of the protoplanetary disk. When x = 1, the critical orbit is in $r \sim 20\ R_J$ in the circumplanetary disk around a Jupiter-like planet with the mass of $0.4\ M_J$. However, when x = 0.1, the critical orbit is in $r \sim 3\ R_J$. Outside of the critical orbit, large satellitesimals accrete pebbles within their accretion radiuses. The radius expands dramatically when the mass of the satellitesimal reaches 10^{23}-10^{24} g, and the satellitesimal grows rapidly after that.
In conclusion, we paved the way for the formation of satellitesimals in a circumplanetary disk and reveal a rough picture of the pebble accretion by the satellitesimals.

Keywords: Satellite, Satellite formation, Pebble accretion , Circumplanetary disk, Satellitesimal, Gas planet

Accretion of icy pebbles by rocky planetary embryos in cooling protoplanetary disks

Takao Sato[1], *Satoshi Okuzumi[1], Shigeru Ida[2]

1.Department of Earth and Planetary Sciences, Tokyo Institute of Technology, 2.Earth-Life Science Institute, Tokyo Institute of Technology

Standard accretion disk models suggest that the snow line in the solar nebula migrated interior to the Earth's orbit in a late stage of nebula evolution. In this late stage, a significant amount of ice could have been delivered to 1 AU from the outer regions of the disk in the form of mm to dm-sized icy particles called "pebbles." This raises the question as to why the present Earth is so depleted of water.
In this study, we quantify the amount of icy pebbles accreted by terrestrial embryos in a cooling protoplanetary disk assuming that no mechanism halts the pebble flow outside the terrestrial planet forming region. We use a simplified version of the coagulation equation to calculate the formation and radial inward drift of icy pebbles in a protoplanetary disk. The pebble accretion cross section of an embryo is calculated using analytic expressions presented by recent studies. We find that the final mass and water content of terrestrial embryos strongly depends on the radial extent of the gas disk, the strength of disk turbulence, and the time at which the snow lines arrives at 1 AU. The disk's radial extent sets the lifetime of the pebble flow, while turbulence determines the density of pebbles at the midplane where the embryos reside. We find that the final water mass fraction of the embryos falls below that of the present Earth (0.023 wt%) only if the disk's radial extent is 100 AU or less, turbulence is strong at 1 AU, and the snow line arrives at 1 AU later than 2-4 Myr after disk formation. If the solar nebula extended to 300 AU, initially rocky embryos would have evolved into icy planets of 1-10 Earth masses unless the snow-line migration was slow. If the proto-Earth contained water of ~ 1 wt% as might be suggested by the density deficit of the Earth's outer core, it would have been possible for the proto-Earth to form with weaker turbulence and with earlier (> 0.5-2 Myr) snow-line migration.
Reference: Sato, T., Okuzumi, S., & Ida, S. 2016, A&A, in press (arXiv:1512.02414)
Figure: Time evolution of the mass and water fraction of an initially purely rocky embryo of the initial mass of 0.1 Earth mass placed at 1 AU in a cooling protoplanetary disk with the outermost radius of 100 AU. The curves show how the mass and water fraction evolve with time if the snow line reaches 1 AU at different times (0.5, 1, 2, 3, 4, and 5 Myr from left to right) after disk formation. The dashed and dotted lines mark the water fraction of 0.023 wt% (corresponding to the current terrestrial value estimated from the ocean mass) and 1 wt% (a theoretical upper limit on the primordial terrestrial value estimated from the mass deficit of the outer core), respectively. The left, center, and right panels are for turbulence parameters of 10^{-4}, 10^{-3}, 10^{-2}, respectively.

Keywords: snow line, terrestrial planets, water

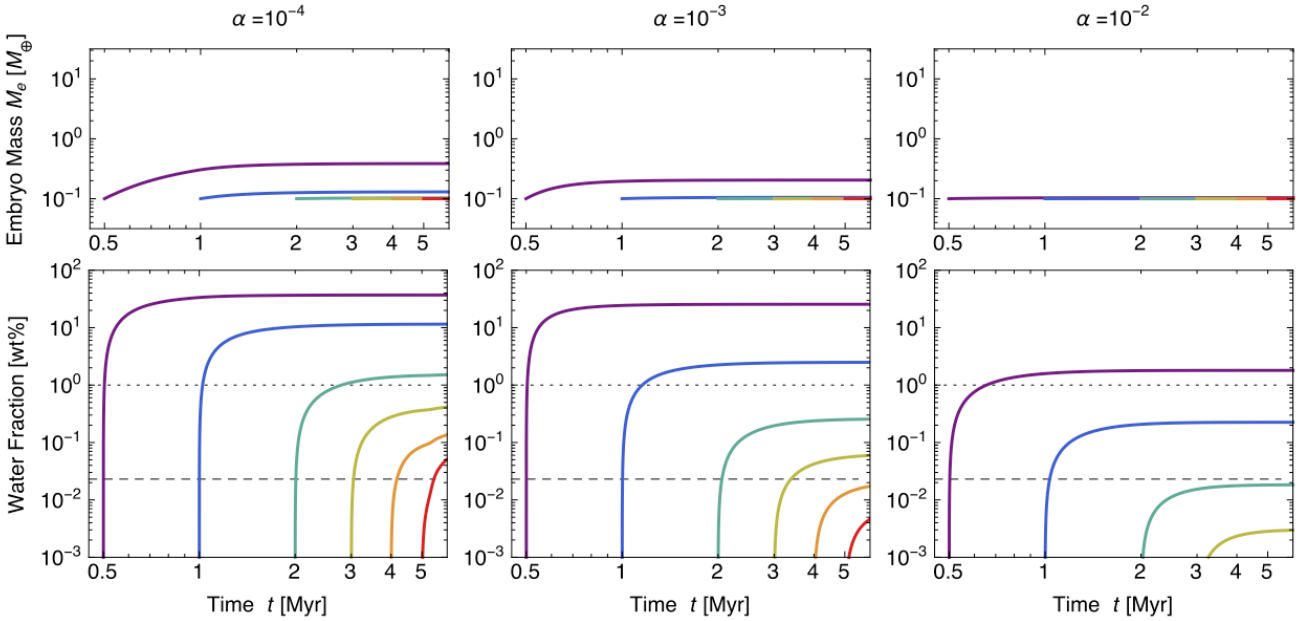

Numerical simulation of collisions between sintered icy dust aggregates

*Sin-iti Sirono[1], Haruta Ueno

1.Department of Earth and Planetary Sciences, Nagoya University

Collision of dust aggregates is a critical step in planetary formation. In the outer regions of a protoplanetary nebula, the main component of a dust grain is ice. Because ice is volatile material, it sublimes and recondenses in a protoplanetary nebula. Dust grains are connected by surface tension, leading to formation of a neck between grains. A neck has a concave surface, in contrast to the other parts of a grain having a convex surface. The equilibrium vapor pressure depends on the shape of surface. A concave surface has a lower vapor pressure than a convex surface. Because the gas pressure is uniform around a dust aggregate, ice molecules sublime from convex surface and recondense on concave surface. This process is called sintering. Sintering induces growth of a neck between grains. A grain can roll against the neighboring grain keeping a connection between grains. This rolling efficiently dissipate the kinetic energy and enables sticking in a collision. However, the rolling requires breakup of a grown neck after sintering. Therefore, it can be expected that sintering strongly affects collisional outcome of icy dust aggregates.
We performed 2-D collision simulations including the effects by sintering. A neck is approximated by an elastic cylinder. The degree of sintering corresponds to the radius of a neck. Head on collisions are simulated. Aggregates without sintering can stick if the collision velocity is less than 50 m/s. We investigated this critical velocity below which collisional growth is possible. When the colliding aggregate is produced by BCCA(Ballistic Cluster Cluster Aggregation) algorithm and sintering degree is high (neck radius/grain radius=0.7), the critical velocity decreases to around 20 m/s. If the degree of sintering is low (neck radius/grain radius=0.2), the necks are broken efficiently and reconnect through non-sintered necks. Then the difference in collisional outcomes is negligible.
When the packing fraction of an aggregate is high, the critical velocity is around 1 m/s. Above this velocity, collisional outcome is bouncing. This is because elasticity of an aggregate is high in this case. The induced stress is higher than the strength of contacting region on the aggregate surface, and the colliding aggregates bounce. When the collision velocity is higher than 20 m/s, Fracturing proceeds around the contacting region and fragments are produced. The amount of fragments is a few % when the collision velocity is 20 m/s.
From these results, sintering hinders collsional growth of icy dust aggregates. Aggregates infall to the central star due to gas drag. Within a sintering region, the infalling velocity differs from that in non-sintering region because the maximum aggregate size is limited by sintering. This velocity contrast produces a contrast in surface density in a protoplanetary nebula. The heterogeneity in solid component might affect planetary formation processes.

Keywords: sintering, dust aggregate, collision

From planetesimals to planets in turbulent protoplanetary disks

*Hiroshi Kobayashi[1], Hidekazu Tanaka[2], Satoshi Okuzumi[3]

1.Department of Physics, Nagoya University, 2.Tohoku University, 3.Tokyo Institute of Technology

In turbulent protoplanetary disks, planetesimals are stirred by turbulence, resulting in orderly growth. As planetesiamls grow via collisions, the escape velocities of planetesimals increase and therefore gravitational forcusing becomes important, which ignites runaway growth. The onset of runaway growth modifies the size distribution of planetesimals; the total mass of planetesimals is in the size of planetesimals at the onset of runaway growth. The planetesimal size determines the final mass of planets and the formation timescale. We deribe the size of planetesimals at the onset of runaway growth as a function of the turbulence strength, the surface density of the disk and distance from the host star. Using the result, we discuss constraints on the solar system formation.

Keywords: planet formation, planetesimal, turbulence

Local numerical simulations of axisymmetric two-dimentional instabilities in the dust layer of a protoplanetary disk

*Isamu Onishi[1], Minoru Sekiya[1]

1.Department of Earth and Planetary Sciences, Kyushu University

Two different processes have been proposed for the formation of planetesimals: mutual sticking of dust aggregates, and the gravitational instability of the dust layer. The critical density of the gravitational instability is hundreds times the gas density. However, the turbulent diffusion may prevent dust particles to settle toward the midplane of the protoplanetary disk, and the condition for the gravitational instability is difficult to be satisfied.

The streaming instability by Youdin & Goodman (2005) concentrates dust particles and boosts the planetesimal formation. The streaming instability is very efficient to form dust clumps in the case where dust particles have the stopping time on the order of the Keplerian orbital period (meter-sized particles). However, the streaming instability grows very slowly for small dust particles (1mm or less).

In this work, we carried out numerical simulations of motions of dust particles and gas in the dust layer of a protoplanetary disk. We assume the axisymmetry with respect to the rotation axis of the protoplanetary disk. We employ the local shearing-box approximation. We take account of the radial tidal force as well as the vertical force due to the stellar gravity, the gas drag force acting on dust particles and its back reaction. We include the effect of global pressure gradient by adding radial force to dust particles. We omit the effects of magnetic fields and the self-gravity.

We use the Athena code developed by Bai & Stone (2010) for numerical simulations. We report the results over a wide range of parameters, and consider comprehensively the causes of the instabilities in the dust layer of a protoplanetary disk.

Keywords: protoplanetary disk, dust, instability, planetesimal

New Condition for The Rossby Wave Instability

*Tomohiro Ono[1], Takayuki Muto[2], Taku Takeuchi, Hideko Nomura[3]

1.Department of Astronomy, Kyoto University, 2.Division of Liberal Arts, Kogakuin University, 3.Department of Earth and Planetary Sciences, Tokyo Institute of Technology

Recent observations have revealed the protoplanetary disks having non-axisymmetric structures, but the origin is still unknown. The Rossby wave instability (RWI) is one of the candidates of the origin. The RWI is a hydrodynamic instability in differential rotation disks, which forms non-axisymmetric large-scale vortices when disk profiles have a rapid radial variation. Previous works propose each of the necessary condition and the sufficient condition for the RWI. However, we are ignorant of the *necessary and sufficient* condition for the RWI.
In this work, we perform linear stability analyses of the RWI for barotropic flow on a wide parameter space. We calculate parameters for marginally stable states to the RWI. We find that the co-rotation radius is located at the background vortensity minimum with large concavity if the RWI is marginally stable. This allows us to check the stability against the RWI easily. We newly derive the *necessary and sufficient* condition for the RWI in semi-analytic form. It is expected that the new condition is available except when the width of the radial variation is much less than the scale height of the disks. The new condition and method will be useful for interpretations of observations and non-linear numerical simulations.

Keywords: protoplanetary disk, hydrodynamic instability, linear stability analysis

Planetesimal Impact Simulations by Godunov SPH Method for Elastic Dynamics with the Effects of Rocks

*Keisuke Sugiura[1], Shu-ichiro Inutsuka[1], Hiroshi Kobayashi[1]

1.NAGOYA UNIVERSITY Graduate School of Science

The earth and other rocky planets are supposed to be formed via collisional coalescences of planetesimals in protoplanetary disks. To understand the origins of rocky planets and characteristic shapes of asteroids we have to study the detail of outcomes of collisions between planetesimals. Laboratory experiments for disruptive collisions have been conducted, but they cannot treat objects larger than several ten centimeters or the velocity higher than several kilometers per second. Hence numerical simulation is powerful and effective method to study planetary collisions.

Many previous works on simulation of planetary collisions have used Smoothed Particle Hydrodynamics (SPH) method, which is one of the computational fluid dynamics methods using Lagrangian particles. However the most popular form of SPH method (the standard SPH method) has several problems. In particular, its spatial accuracy is lower than first order in disordered particle distribution; it utilizes artificial viscosity that tends to cause particle penetration in strong shock waves; the tensile instability, which is numerical instability, occurs in tension-dominated region. Moreover the effects of solids such as deviatoric stress are generally ignored in protoplanet collisions mostly in cases where self-gravity is dominant. The influence of the effects of solids for large protoplanet impacts is not fully discussed. Thus we should consider those effects, which requires us to develop an appropriate numerical simulation method.

Godunov SPH method (Inutsuka 2002) is proposed to solve the problems in the standard SPH method. The Godunov SPH method achieves second-order accuracy in space. To avoid the use of artificial viscosity it uses Riemann solver, which can introduce (possibly) minimum but sufficient physical viscosity. Moreover the Godunov SPH method can solve the tensile instability by selecting appropriate order of interpolation that is used in the equation of motion (Sugiura and Inutsuka 2016). We further extend the Godunov SPH method to elastic dynamics, and implement several models represent the effects of realistic solid material such as fracture. In this talk, we show the results of numerical simulations for planetesimal collisions that account for the effects of solid material, and discuss its influence.

Keywords: Planetesimals, collisional destruction, numerical simulation, elastic dynamics , Godunov SPH method

Scaling of impact-generated cavity-size for highly porous targets and its application to cometary surfaces

*Takaya Okamoto[1], Akiko Nakamura[2]

1.Planetary Exploration Research Center, Chiba Institute of Technology, 2.Department of Planetology, Graduate School of Science, Kobe University

Recent spacecraft missions have brought us the information of highly porous small bodies. The detail images of these bodies show variety of the surface. One of the interesting findings is that the depressions on comets look shallower than the simple craters such as on the moon, that is the depth-to-diameter ratio of the depressions are smaller than ~0.2. Although the mechanisms for the formation of the depressions such as collapse after the sublimation of the sub-surface volatile (Vincent et al., 2015) and activities after impact such as sublimation and viscous relaxation (e.g. Cheng and Dombard 2006, Thomas et al., 2013) are controversial, the shape of the cavity formed on highly-porous surface by impact itself is not understood well.
We performed impact experiments of sintered glass-bead targets with porosity of ~94%, and 87%, as well as gypsum targets with porosities of ~50% and pumice targets with those of 74%. The cavity created by the impact has maximum diameter at some depth from the target surface. The shape of the cavity is called bulb-shape cavity (Okamoto et al., 2013).The maximum diameter, D_{max} and the bulb depth, d_b of the cavity were analyzed. In addition to the results of this study, we also compiled the results of previous impact experiments for crater sizes in which the targets with porosity larger than 30% were used. Then new empirical scaling relations for the wide range of target porosity were obtained.
We applied the relations to comets. The surface strength and the particle size of the comet Tempel 1 are estimated to be of the orders of 10^1–10^3 Pa, and larger than ~50 μm, respectively. The ratio of bulb depth to the maximum diameter is also calculated from the scaling relations. The results show that the ratio on the weak surface with the strength less than 100 Pa was smaller than the depth-to-diameter ratio of simple craters, ~0.2. It suggests that shallow depressions on comets could be formed only by impact without subsequent activities, such as sublimation and viscous relaxation.

Keywords: porosity, hypervelocity impact experiment, comets

Cratering on iron alloy: Temperature and impact velocity effe cts

*Ryo Ogawa[1], Akiko Nakamura[1], Ayako Suzuki[2], Sunao Hasegawa[2]

1.Graduate School of Science, Kobe University, 2.Institute of Space and Astronautical Science

Introduction: Planetary differentiation could occur on planetesimals with diameters more than 20 km to form iron cores (Moskovitz and Gaidos, 2011). It is noted that the core formation occurred 0.3-0.6 million years after the most primitive material "CAI" was formed (Kruijer et al., 2014). That is, the core formation is a very primitive event and important to understand the early stage of the planetary evolution.
Currently, much attention is paid to an M-type asteroid 16 Psyche. Psyche may be the exposed iron core of a protoplanet and the Psyche orbiter mission is one of five Discovery Program semifinalist proposals. In order to get better understanding of planetary formation and evolution through such space mission, we have to understand about impact process on the surface of iron bodies. We performed impact experiments and simulations and examined the effects of temperature, impact velocity, on a cratering on iron material to collect basic data and examine model parameters (Ogawa et al., Shototsu Kenkyukai (in Japanese) 2016). In this study, we performed impact experiments and simulations with copper projectile which has well-defined material parameters to examine the effect of the projectile material. Furthermore, we performed numerical simulations of planetary scale cratering and compared them with the laboratory-scale ones.
Experimental method: We performed impact experiments with velocities of 6.8-7.3 km/s under 0.5-5.0 Pa using a two-stage light-gas gun at the Institute of Space and Astronautical Science (ISAS). Our targets were iron alloy (SS400) cubes with 50 mm each side. Projectiles were copper spheres of 3.2 mm in diameter. We used room-temperature (298 K) and low temperature (150 K) targets. The target material has brittle-ductile transition temperature at about 200 K. We simulated the cratering on the iron alloy using a shock physics code "iSALE" under the same conditions as the experiments. We used the Johnson-Cook strength model parameters of oxygen-free copper (Johnson and Cook, 1983) for projectiles and SS400 which we determined in our previous study for the targets. Moreover, we simulated planetary scale impacts with the stainless steel impactors of 0.02-5 km in diameter and SS400 targets of 0.2-200 km in diameter and examined the effect of the size using PI scaling.
Results of experiments: The craters of the low-temperature targets were shallower than the room-temperature targets at low impact velocity (2 km/s). However, the effect of temperature on depth couldn't be seen at high velocity (4-6.5 km/s). Moreover, we also couldn't find the effect of the temperature on diameter. Some of the iron alloy's strength increases by cooling (e.g. Petrovic, 2001). Therefore, the craters on the room-temperature targets were deeper than the low-temperature targets. On the other hand, the adhesion of the projectiles on the craters were seen in the experiments and simulations. In order to explain why the effect of temperature on depth wasn't seen at high impact velocity, we have to examine other effects than the strength-increase by cooling.
Results of simulations: The effect of temperature on the crater depth was less than those of the experiments. We haven't found why but it might be because the copper's Johnson-Cook parameters were 1/3-1/5 of those of SS400. A comparison between the simulation and laboratory results using PI scaling shows that craters were deeper in planetary scale than laboratory-scale at low impact velocity. Moreover, the craters on the low-temperature targets were as deep as room-temperature targets in planetary scale.

Keywords: Iron, Crater, Impact

Experimental estimate of mass loss rate by cratering for rubble-pile asteroids

*ERI TATSUMI[1], Seiji Sugita[1]

1.The University of Tokyo

Both Ground-based and spacecraft observations suggest that many small asteroids (< 10 km) have rubble-pile structures based on spin-rate, density, and geological features [1]. Recently theoretical study indicated that cratering might play a decisive role for size-frequency distribution of the main-belt asteroids besides catastrophic disruption [2]. Cratering on rubble-pile targets, which are loosely combined by small gravities and/or cohesions, has not been fully understood, although there are a few sets of experiments [3]. In this study, we conducted impact experiments to construct new scaling law for coarse-grained targets simulating the rubble-pile asteroid surfaces.
Impact experiments: We used two vertical guns in the Univ. of Tokyo and ISAS, for impact velocities 79 - 224 m/s and 1 - 6 km/s, respectively. We used polycarbonate projectiles 0.76 - 0.77 g for the former gun and 0.068 g for the latter gun. Pumice blocks (~7, 9, and 16 mm), basalt blocks (~ 10, and 18 mm) are used as boulder target simulants. The cross-section profiles were obtained by a laser profiler (Keyence, LJ-V). In order to observe the cross-section during cratering, we also conducted quarter-space experiments and recorded by a high-speed camera (NAC, Q1v).
Results and analyses: If target grain sizes do not influence cratering, crater sizes are the same sizes on sand targets. However, our results suggested that although high-velocity impacts (>4 km/s) formed similar crater sizes as sand targets, low-velocity impacts (<4 km/s) resulted in smaller craters than sand targets. This is because energy dissipation by target grains disruption is not negligible compared to excavation energy. The trend of our results can not be explained by the classic πscaling by [4]. Quarter-space experiments suggest that cratering on coarse-grained targets would be divided into two stages: an early disruption stage and a latter excavation stage. We modified the scaling law based on the quarter-space observation, assuming that the momentum of an impactor transferred to a contacted target grain immediately, that is when a target grain size is larger than an impactor size, the effective velocity that controls the excavation field would be smaller. Using the new modified scaling law, we can estimate crater sizes on real-sized bodies.
Implications for mass loss rate: For example, on Itokawa (average surface grain size of 2 m) impactors smaller than 1 m might result in smaller craters than sand targets by 5 times at most and impactors smaller than 0.1 m rarely cause crater because they do not have enough energy to disrupt surface grains. In contrast, impactor larger than 1 m could form craters as large as craters on sand targets. When an impactor can fully disrupt a target grain, a crater is at least several times larger than a crater on rigid bodies such as rocks. Thus, the cratering mechanisms on large continuum asteroids and small rubble-pile asteroids might be very different. The mass loss on cratering could be assessed by the classic scaling law if the latter excavation mechanism is the same as cratering on sand targets. The rubble-pile asteroids can lose their mass easily compared to the same-sized rigid bodies due to larger craters. Resent observations of the small-main-belt asteroids suggest that smaller asteroids are depleted from the steady distribution decided by the catastrophic disruption with the slope of -3.5 (e.g., [5]). The high efficiency of mass loss among rubble-pile asteroids might be responsible for the lack of small asteroids.
[1] Pravec and Harris, Icarus 148, 12-20 (2000); Britt et al., Asteroids III, 485-500 (2002); Fujiwara et al., Science 312, 1330-1334 (2006) [2] Kobayashi and Tanaka, Icarus 206, 735-746 (2010) [3] Güttler et al., Icarus 220, 1040-1049 (2012); Holsapple and Housen, 46th LPSC, #2538 (2014) [4] Holsapple, Annu. Rev. EPS 21, 333-373 (1993) [5] Gladman et al., Icarus 202, 104-118 (2009)

Keywords: Asteroids, Impact experiments, Crater

Experimental study on propagation process of impact-induced seismic wave in quartz sand simulating asteroid regolith layer

*Kazuma Matsue[1], Masahiko Arakawa[1], Minami Yasui[1], Shota Takano[1], Sunao Hasegawa[2]

1.Graduate School of Science, Kobe University, 2.Institutes of Space and Astronautical Science, JAXA

Planetary explorations in the solar system have revealed that the asteroid surfaces were covered with the regolith layer made of boulders and granular materials. The surface morphologies of asteroids formed on the regolith layer were recently proposed to be modified due to the impact-induced seismic activity. Then, it is important for us to understand the physical mechanism of the impact-induced seismic vibration. Therefore, we carried out impact cratering experiments on quartz sand using a polycarbonate projectile to observe the seismic wave propagating through the sand (Matsue, (JPGU 2015)). Recently, we established a sabot-stopper method to launch various kinds of projectiles at a vertical type two stage light gas gun, then we performed the high-velocity impact experiments using a projectile made of different materials with the diameter of 2mm, and measured the impact-induced seismic wave. Based on the result of this study, we examined the attenuation rate of seismic wave in the quartz sand and the energy partition rate between the projectile kinetic energy and the kinetic energy of the seismic wave.
Impact cratering experiments were conducted by using a single stage vertical gun set at Kobe University and a two-stage vertical gun set at Japan Aerospace Exploration Agency (JAXA). The impact velocity was 0.2-6.9km/s using a polycarbonate projectile and 2,4,5km/s using a projectile made of different materials with a diameter 2mm: glass, aluminum, titanium, zirconia, stainless steel, copper and tungsten carbide. We used a quartz sand target with the particle diameter of 500μm and the bulk density of 1.48g/cm^3. The accelerometers were set on the target surface at different distances from the impact point. After each experiment, we measured the crater profile by using a laser profiler in order to acquire the crater shape quantitatively.
The crater shape formed by the polycarbonate projectile at different impact velocities showed the similarity, irrespective of the velocity, however the similarity was not followed by the results obtained by the projectile with different densities. Then, we found that the ratio of the crater depth to the diameter (d/D) was not constant and depended on the projectile density. On the other hand, the crater size is expressed by the π-scaling law. The impact induced seismic wave was classified into two categories according to the distance from the impact point: at the region far from the impact point, the seismic wave looks like a damped vibration wave, and at the region near the impact point, the seismic wave looks like a single pulse wave. It is noticeable that the peak value of the acceleration changes with the propagation distance: the maximum acceleration, g_{max}, has a power law relationship to the normalized distance x/R, where x is propagation distance and R is crater radius as follows, $g_{max}=10^{2.2\pm0.04}(x/R)^{-3.11\pm0.11}$. We calculated the impact-induced seismic efficiency factor, k; that is, the ratio of the impact-induced seismic energy to the kinetic energy of the projectile. The impact-induced seismic energy was assumed to be the kinetic energy of the quartz sand vibrating at the thin shell region with a width corresponding to one cycle of the seismic wave. As a result, the average of k was obtained to be $(8.1 \pm 5.0) \times 10^{-5}$ for the polycarbonate projectile impacts.

Keywords: crater, regolith layer, seismic shaking

Impact-driven flow-field: Hypervelocity material ejection from the interference zone

*Kosuke Kurosawa[1], Takaya Okamoto[1], Hidenori Genda[2]

1.Planetary Exploration Research Center, Chiba Institute of Technology, 2.Earth-Life Science Institute, Tokyo Institute of Technology

The scaling relationship of the excavated mass at a bin of ejection velocity has been widely explored to understand the effect of hypervelocity impacts on the material distribution on the planetary surface. The high-velocity component from the vicinity of the impact point, however, has not been investigated well probably because the mass of high-velocity component is likely to be a few orders of magnitude lower than the entire mass of impact ejecta. Nevertheless, such high-velocity component would mainly contribute to the material exchange between planets/satellites and the production of unique samples in strata on the Earth via aerodynamic heating during their flight in the atmosphere because there is a threshold velocity in such problems.
We meet three difficulties in the problems. Among them are (1) The point-source approximation cannot be applied because the excavation flow is expected to be driven by a shockwave generated during a projectile penetration, (2) a propagating shockwave interacts with a rarefaction wave from the free surface, leading to produce a complex flow field, which is referred to as the interference zone, and (3) the flow field cannot be solved analytically because of the non-linear nature of such flow field. Although Melosh (1984) approximately estimated the thickness of the interference zone and the ejection velocity under several assumptions, his model cannot be directly applied to the vicinity of the impact point within ~2-fold impactor foot print as pointed out by himself.
In this study, we analyzed such complex flow field using the iSALE shock physics code to obtain the highest velocity form the target surface. For simplicity, we calculated only vertical impacts. A cylindrical coordinate was employed. We used the Tillotson EOS for granite to treat the effects of thermal pressure due to irreversible shock heating on the change in the particle velocity. Although we assumed a spherical projectile with 10 km in diameter for reasons of expediency, the results can be converted to any size of projectile through appropriate scaling calculations because we did not include material strength and gravity in this calculation. The impact velocity was set to 12 km/s, which is a typical value of that to Mars and the Moon. Lagrangian tracer particles were inserted into each computational cell to obtain the change in the position, pressure, and energy as a function of its initial position. We analyzed the particles ejected within 3 seconds after the impact.
The particle motions are qualitatively consistent with the predictions by Melosh's model. It is important that the incidence angles of the shockwave and the rarefaction wave become nearly perpendicular in the interference zone. Thus, the accelerated materials by the shockwave suffer a further acceleration due to rarefaction wave in the upward direction. At this time, the stored internal energy due to the shock heating is converted to the kinetic energy of the upward motion. The highest ejection velocity determined by such acceleration is ~2-fold particle veloctity at the shocked state, which can be calculated using the Rankine-Hugoniot relations. Numerical calculations allow us to investigate the peak pressure at each position in the interference zone. The highest ejection velocity under the condition is ~5.5 km/s, which is about half of the impact velocity. The ejected mass at higher than 5 km/s is ~0.1 wt% of the projectile mass and they suffer the peak pressure of 40 GPa.
We are planning to do a series of numerical calculations to obtain the velocity-mass relation of the ejecta from the interference zone.

Keywords: Hypervelocity impacts, Impact ejecta, Martian meteorite

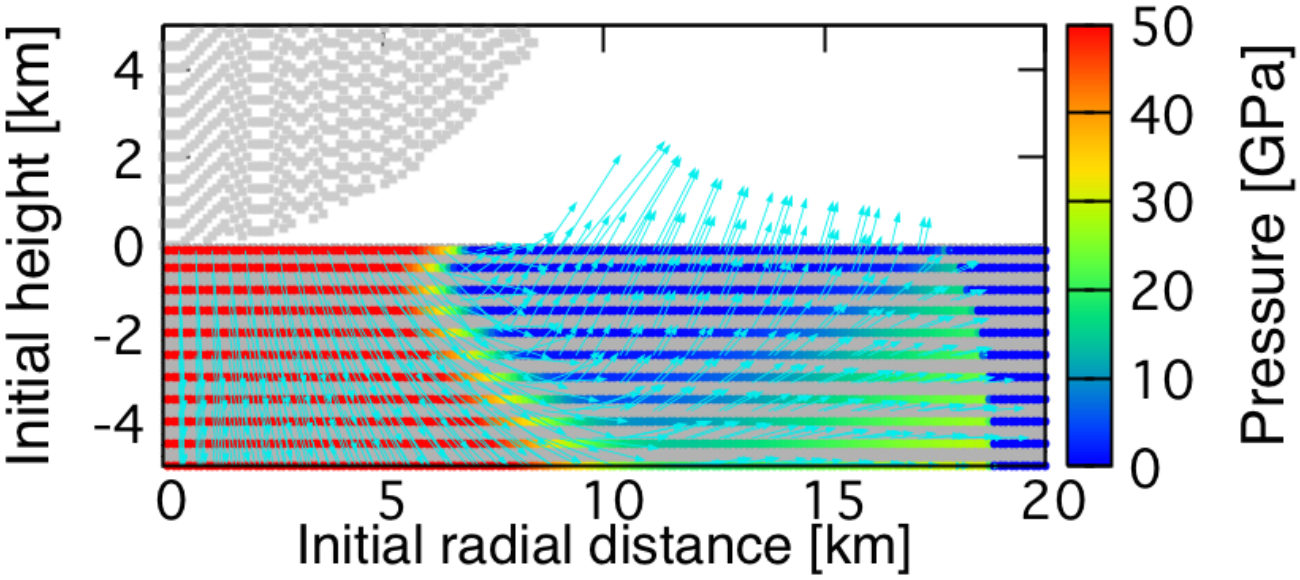

Water Partitioning into the Martian Mantle during Accretion of Mars

*Hiroaki Saito[1], Kiyoshi Kuramoto[1]

1.Department of Cosmosciences, Graduate School of Sciences, Hokkaido University

According to the latest analyses of Martian meteorites, the early Martian mantle was possibly wet with the H_2O concentration to be 780 ~ 2870 ppm (McCubbin et al., 2012). This estimate is equivalent to about 0.3~1 times the Earth ocean mass (~1.4×10^{21} kg) in the whole Martian mantle. Because of the lack of plate tectonics on Mars, water is likely to be partitioned to the interior during accretion of Mars. A planetary-scale magma ocean produced by the accretion energy and/or the blanket effect of the proto-atmosphere possibly absorbs a vast amount of water. However, it remains an open question how such a magma ocean could be formed on accreting Mars.
The precise Hf-W chronology suggests that the growth of Mars had been almost completed within the first several Myr after the formation of CAI (Dauphas and Pourmand, 2011: Tang and Dauphas, 2013), which is consistent with the theoretical estimate for the formation time of proto-planets. During such rapid accretion, a proto-Mars might gravitationally keep both degassed component and the solar nebula component as a proto-atmosphere. We call this atmosphere hybrid-type proto-atmosphere.
In this study, we analyze the thermal structure of hybrid-type proto-atmosphere by developing a 1D radiative-equilibrium model. Here we take into account the effect of the possible reduction of solar nebula pressure during accretion, taking the original nebula pressure at the Hill sphere to be 6.9×10^{-2} Pa (p_0) (Kusaka et al., 1970) and the minimum nebula pressure to be $10^{-12}\times p_0$. The accretion time is varied from 1 to 6 Myr so as to meet the chronological constraints. The building blocks of Mars is modeled by applying the two-component model (Wanke and Dreibus, 1988), which contains 35% of volatile-rich, oxidized CI chondritic material and 65% of volatile-poor, reduced E chondritic material. Impact degassing occurs for the planetesimal impacts with sufficiently high velocity as the growing Mars exceeds 0.1 times the final mass. Degassed volatile has a composition determined by the chemical equilibrium with molten silicate and metal produced by impact shock heating. Degassed component is assumed to occupy the lower atmosphere below the hydrogen-helium upper atmosphere continued to the solar nebula at the Hill radius.We solved the evolution of hybrid-type atmosphere with the growth of a proto-Mars. Independent of accretion time and nebula dissipation timescale, the proto-atmosphere is so massive and hot enough to produce the magma ocean during the last half stage of accretion. In the case without nebula dissipation, the surface pressure exceeds the solidus temperature 1500K of rock as the proto-Mars has grown larger than 0.3 times the final mass, and the surface pressure reaches ~2000bar at the end of accretion. On the other hand, in the case of lowered nebula pressure, the beginning of surface rock melting delays until the proto-Mars becomes larger than ~0.6 of its final mass due to the partial loss of degassed component to space, but the surface pressure still reaches ~ 800bar at the end of accretion. The amount of water partitioned into the magma is estimated to be ~9.6×10^{20} kg or larger. This value is equivalent to ~0.7 Earth ocean mass, which is basically consistent with the petrological evidence.

Keywords: Early Mars, Magma Ocean, Wet mantle

Diversity of atmospheric circulations of tidally locked gas giant planets -- dependence on the incident radiation strength

*Shin-ichi Takehiro[1], Yoshiyuki O. Takahashi[2], Kensuke Nakajima[3], Yoshi-Yuki Hayashi[2]

1.Research Institute for Mathematical Sciences, Kyoto University, 2.Department of Earth and Planetary Sciences, Kobe University, 3.Department of Earth and Planetary Sciences, Kyushu University

Thanks to recent development of observational instruments, the number of discovered exoplanets has been surprisingly increased. In particular, it is considered that there are many tidally locked gas giant planets, whose same hemispherical surfaces face to the central stars (hot Jupiter). General circulations of the surface atmospheres of such gas giants have been investigated using simplified and modified models for the Earth's atmospheric general circulation. One of the prominent characteristics of these simulations presented so far is a strong equatorial prograde jet (equatorial superrotation). However, the condition emerging a equatorial prograde jets is not well understood. Our purpose is to make clear the regimes of atmospheric general circulations of tidally locked gas giant planets through a series of numerical experiments using general circulation models where the parameters of the planetary atmospheres are widely varied, and understand diversity of atmospheric circulations of tidally locked gas giants. In this study, we investigate dependence on the incident radiation strength.
The atmospheric model used for numerical experiments is "DCPAM5" developed by GFD Dennou Club (http://www.gfd-dennou.org/library/dcpam/), which is a three-dimensional primitive model assuming hydrostatic balance in the radial direction. Dual band radiative transfer is adopted to express incident short wave radiation and outgoing long wave radiation. The incident radiation from the central star illuminates only the same hemisphere of the planet at all times. There is no heat flow through the bottom boundary. The parameters characterizing the planetary atmosphere in the model are based on those of the exoplanet HD209458b. Incident radiation strength is varied around the value of HD209458b. Time integrations are performed for various strength of incident radiation. When the incident radiation is as strong as that of the original HD209458b (10^6 W/m^2), strong equatorial prograde jet emerges which penetrates to about 1bar level. The equatorial jet is weakened and becomes shallow as the incident radiation is decreased. Finally, when the incident radiation is as weak as 10^3 W/m^2, equatorial zonal flows tend to retrograde and prograde high latitude jets become dominant. The newly found equatorial retrograde regime of tidally locked gas giants contrasts with that of equatorial prograde flow proposed so far.

Keywords: Hot Jupiter, Equatorial jets, Equatorial superrotation

A New Microphysical Model for Exoplanetary Clouds: Testing against the Observations of Terrestrial and Jovian Clouds.

*Kazumasa Ohno[1], Satoshi Okuzumi[1]

1.Department of Earth and Planetary Science, Graduate School of Science and Technology, Tokyo Institute of Technology

Recent transit surveys have shown that some close-in exoplanets have a featureless transmission spectrum. These planets are commonly thought to have high either an atmosphere with a high molecular weight or an optically thick dust cloud at a high altitude. A realistic exoplanetary cloud model is necessary to understand which interpretation is more likely for each exoplanets. Previous cloud models involve some free parameters whose relationship with the microphysics of the formation and growth of cloud particles is unclear. Furthermore, some models neglect the coalescence of dust cloud particles by assuming that micron-sized dust particles are unable to stick in an updraft.

We have been developed a new exoplanetary cloud model that involves the microphysics of condensation and coalescence (the Meeting of The Japanese Society for Planetary Sciences 2015). Our model produces the vertical distributions of the number and mass densities of cloud particles as a function of the atmospheric updraft velocity, the mixing ratio of the condensing gas at the cloud deck, and the number density of cloud condensation nuclei (CCN).

Here, we test the validity of our model by comparing with the observations of the clouds on the Earth and Jupiter. For terrestrial water clouds, we find that our model plausibly reproduces the cloud optical depth from satellite observations and vertical distributions of the mass and number densities of cloud particles from in situ observations. For Jovian ammonia clouds, our model simultaneously reproduces the particle effective radius, cloud optical depth, and cloud geometric thickness from far-infrared observations by assuming the updraft velocity of 1.2–2 m/s and CCN number density of ~5×10^{4} m^{-3}. The parameters values assumed for the Jovian clouds are consistent with the Galileo probe observation and with previous 2D simulations of moist convection in the Jovian atmosphere.

Keywords: exoplanet, cloud

A numerical experiment on occurrence condition of the runaway greenhouse state with a atmospheric general circulation model

*Masaki Ishiwatari[1], Satoshi Noda[2], Kensuke Nakajima[3], Yoshiyuki O. Takahashi[4], Shin-ichi Takehiro[5], Yoshi-Yuki Hayashi[4]

1.Faculty of Science, Hokkaido University, 2.Graduate School of Science, Kyoto University, 3.Department of Earth and Planetary Sciences,Flculty of Sciences,Kyushu University, 4.Graduate School of Science, Kobe University, 5.Research Institute for Mathematical Sciences, Kyoto University

Aiming for assessing the potential habitability of extrasolar terrestrial planets, the existence condition of liquid water on planetary surfaces has been discussed (e.g., Kasting et al., 1993). One of the main issues is the examination on the occurrence condition of the runaway greenhouse state. The runaway greenhouse state is defined as a state in which incident flux given to the atmosphere exceeds the radiation limit: the upper limit of outgoing longwave radiation (OLR) emitted from the top of the moist atmosphere on a planet with ocean (Nakajima et al., 1992). In the runaway greenhouse state, thermal equilibrium cannot be realized. Recent studies utilizing atmospheric general circulation models (AGCMs) discuss that atmospheric circulation and cloud albedo significantly affect the occurrence condition of the runaway greenhouse state (e.g., Leconte et al., 2013; Yang et al., 2013; Wolf and Toon, 2015). However, our speculation is that the runaway greenhouse state emerges when global mean absorbed solar radiation flux exceeds the maximum values of OLR. In order to confirm our speculation, we perform a numerical experiments with an AGCM. We examine the response of modeled atmospheric states to the increase of solar flux considering two spatial and temporal distributions: one for synchronously rotating planets with fixed dayside and nightside, and the other for an Earth-like, non-synchronously rotating planets with diurnal and seasonal changes. We use the AGCM developed by our research group, DCPAM (http://www.gfd-dennou.org/library/dcpam). Subgrid physical processes are parameterized with standard methods used in terrestrial Meteorology. The amount of cloud water is calculated with integrating a time dependent equation including generation, advection, turbulent diffusion, and extinction of cloud water. Extinction rate of cloud water is assumed to be proportional to the amount of cloud water, and extinction time is given as an external parameter. The entire surface is assumed to be a ``swamp ocean'' with zero heat capacity. The results of our experiment show that horizontal deviation of OLR decreases with increasing the value of solar constant regardless the radiation scheme (grey scheme or non-grey scheme), existence of clouds, and solar flux distribution. It seems that runaway greenhouse state appears when global mean absorbed solar radiation flux exceeds the maximum values of OLR. Our results suggest that the occurrence condition of the runaway greenhouse state is determined by a common mechanism, although the maximum value of OLR differs among runs with different conditions.

Keywords: runaway greenhouse state, exoplanet, radiation limit, atmospheric general circulation model, habitability

Two humidity regimes of stratosphere on a moist atmosphere

*Masanori Onishi[1], George HASHIMOTO[2], Kiyoshi Kuramoto[3], Yoshiyuki O. Takahashi[1], Masaki Ishiwatari[3], Yasuto TAKAHASHI[3], Yoshi-Yuki Hayashi[1]

1.Graduate School of Science, Kobe University, 2.Graduate School of Natural Science and Technology, Okayama University, 3.Graduate School of Science, Hokkaido University

An inner edge of habitable zone is characterized by runaway greenhouse limit and water loss limit. Kasting et al. (1993) and Kopparapu et al. (2013) estimated these limits by one-dimensional radiation transfer model. These studies assumed the isothermal atmosphere at 200K. This assumption, however, has a significant effect on the water loss limit because the limit is depend on the temperature of cold trap.Kasting et al. (2015) estimated the temperature profiles on planets with N_2, CO_2 and H_2O atmosphere by one-dimensional radiative-convective model. Their calculations suggest that the water loss limit can be estimated by an isothermal model, provided that one uses a stratospheric temperature of 150 K. Leconte et al. (2013) and Wolf & Toon (2015) calculated the temperature profiles by GCM and estimated that the stratosphere temperatures ware 140 ~ 150 K. These models used k-distribution method.Arking & Grossman (1972) estimated the temperature profiles of radiative equilibrium state by using an idealized semi-analytical non-grey radiative model. This study showed that in a non-grey atmosphere, the temperature increases with increasing mean opacity below a certain height and decreases with increasing mean opacity above that height. It also found that there is no lower limit to the temperature at the top of the atmosphere: it can approach zero arbitrarily closely as the width of the lines is decreased. This result implies that estimating temperature of upper part of atmosphere needs a high resolution calculation.In the temperature profiles estimated by previous studies, tropopause pressure is much lower than that in present-day Earth: 1000 ~ 1 Pa. On the other hand, these studies used the modified models from present Earth models. To estimate the temperature of higher tropopause, a radiative transfer model which calculates opacity of each wavelength accurately enough for estimating temperatures in lower pressure tropopause than that of Earth is required. We estimate the temperature by using such a one-dimensional, line-by-line radiative transfer model. The model atmosphere is assumed to consist of H_2O and N_2. The troposphere and stratosphere is assumed to be fully saturated and isothermal, respectively. The value of a heating rate in tropopause are calculated for various surface and tropopause temperatures. The wavenumber resolution of this model is 10^{-4} cm^{-1}, in 0 –3000 cm^{-1}; 10^{-2} cm^{-1}, 3000 –76576 cm^{-1}. The result shows the existence of two regime: one is dry regime, and the other is wet regime. In a dry regime, the tropopause temperature is about 120 K, that is independent of surface temperature. A wet regime, in which water vapor becomes a major constituent, appears when the surface temperature is higher than 345 K. The model atmosphere does not experience a water loss phase, instead skipping directly to a runaway greenhouse.

Keywords: moist atmosphere, radiative property, habitable zone, water loss limit

Search for Earth-like planets around late-M dwarf stars using the infrared Doppler

*Masashi Omiya[1,2], Takayuki Kotani[2,1], Motohide Tamura[3,2,1]

1.National Astronomical Observatory of Japan, 2.AstroBiology Center, 3.The University of Tokyo

We are proposing to conduct a strategic infrared Doppler survey for extrasolar Earth-like planets around M dwarf stars using a new astronomical infrared instrument (InfraRed Doppler instrument, IRD) for the Subaru telescope at Hawaii. For very precise radial velocity measurements in the infrared wavelength, IRD is composed of a stable astronomical high dispersion spectrograph and a laser-frequency comb as a precise wavelength calibrator covering the range of 0.97-1.75 micron. The main goals of the IRD survey are to achieve a radial velocity precision of 1m/s for late-M dwarfs and to search for Earth-like exoplanets around low-mass stars. Planetary systems around low-mass stars are attractive targets to detect extrasolar Earth-like planets in the habitable zone by the Doppler method because of relatively large signals caused by the planets and their close-in habitable zone. For the advantages of IRD and late-M dwarfs, we plan to perform a new unique large-scale planet search program to look for Earth-like planets by the Doppler method using the IRD and the Subaru telescope.
We have a plan to perform the first light of IRD in this summer and start the full-scale Doppler survey. In this survey, we would like to have 170 observing nights for 5 years from 2017 and observe ~100 carefully-selected late-M dwarfs. We performed a detailed survey simulation and target selection of suitable stars for the survey based on the theoretical simulation and real observation schedule. We will expect the discovery of more than 10 Earth-like planets in the habitable zone and more than 50 exoplanets for the survey period of 5 years. In this presentation, we report the current status of the construction and the observation plan and discuss expected detectable Earth-like planets and impacts on the exoplanet study in the Subaru/IRD survey.

Keywords: Earth-like planets, late-M dwarf stars, Infrared Doppler observation

Constraints on atmospheric pressure on early Mars inferred from nitrogen and argon isotopes

*Hiroyuki Kurokawa[1], Kosuke Kurosawa[2], Tomohiro Usui[3]

1.Earth-Life Science Institute, Tokyo Institute of Technology, 2.Planet. Explor. Res. Ctr., Chiba Institute of Technology, 3.Dept. of Earth & Planet. Sci., Tokyo Institute of Technology

Geomorphological evidence such as valley networks and deltas on Mars requires repeated episodes of liquid water runoff in the Noachian period. A dense atmosphere possibly caused water-ice being transported to the highlands. Fluvial terrains can be created by episodic melting events of ice under such conditions [1]. The dense atmosphere was lost from Mars, but the mechanism and timing are poorly constrained.
We constructed a one-box atmosphere-hydrosphere model with multiple species (CO_2, N_2, H_2O, and noble gases). We calculated the evolution of the volume and isotopic composition of the Martian atmosphere taking into consideration several processes, including impacts of asteroids and comets, atmospheric escape induced by solar radiation and wind, volcanic degassing, and a gas emission from interplanetary dust particles. A threshold for the atmospheric collapse (0.3 bar) was assumed following recent 3D global-circulation-model simulations [e.g., 2]. Comparing our results with nitrogen and argon isotopic compositions at 4.1 Ga recorded in Allan Hills (ALH) 84001 provided a lower limit of the atmospheric pressure on early Mars.
Since impacts mainly contribute to the evolution of atmosphere during the late accretion at 3.5-4.5 Gyr ago, the atmospheric pressure evolved stochastically for the first ~1 billion years. The atmospheric evolution depends on the volatile abundances in the impactors. In cases where relatively volatile-poor impactors were assumed, the impact erosion prevailed over the injection of volatiles and the atmospheric collapse occurs during this period.
Whereas the nitrogen ($^{15}N/^{14}N$) and argon ($^{38}Ar/^{36}Ar$) isotopic ratios kept unfractionated values before the collapse, they increased stochastically after the collapse. Impacts of asteroids and comets in a thinner atmosphere increased abundances of nitrogen and argon. It resulted in higher escape rates of these species and subsequently increased their isotope ratios. The cases of a moderately dense atmosphere (> 0.3 bar) at 4.1 Ga are consistent with unfractionated nitrogen and argon isotope ratios recorded in ALH 84001 [3]. This lower limit of the atmospheric pressure is valid regardless of the presence/absence of the Martian magnetic dynamo at 4.1 Ga because the atmospheric nitrogen was removed by photochemical escape driven by solar radiation.
The reported data on the trapped-nitrogen-isotope composition of ALH 84001 are highly scattered (~7 per mil to >200 per mil) in the literature. Identification of the actual nitrogen isotope ratio at 4.1 Ga would help to constrain the evolution of the Martian atmosphere.
Our results provided a lower limit of the atmospheric pressure at 4.1 Ga. If we combine our results with other constraints on the atmospheric pressure on early Mars [4], a moderately dense atmosphere (~0.1-1 bar) was suggested. We suggest that the moderately dense atmosphere was lost after 4.1 Ga by the impact erosion and the escape induced by solar radiation and wind.

[1] Wordswort, R. et al. (2013) Icarus, 222, 1-19. [2] Forget, F. et al. (2013) Icarus, 222, 81-99. [3] Mathew, K. J. & Marti, K. (2001) J. Geophys. Res., 106, E1, 1401-1422. [4] Kite, E. S. et al. (2014) Nature Geosci., 7, 335-339.

Keywords: Mars, Atmosphere, Isotopes

Shooting star formation in a laboratory experiment

*Hiroki Senshu[1], Kosuke Kurosawa[1], Takaya Okamoto[1]

1.Planetary Exploration Research Center, Chiba Institute of Technology

A shooting star is caused by an entry of a cosmic dust particle into the planetary atmosphere. The light from the shooting star composed of thermal emission and emission lines from the gas in from of the dust particle and the vapor from the dust particle. It means that the physical and chemical condition of the dust particle can be estimated from a photometric and/or spectroscopic observations. However a shooting star is a sporadic and un-controled event, and thus the relation between the physical and chemical condition and the resulting spectroscopic observation is estimated by empirical equations.
We are constructing a laboratory experimental system to simulate shooting stars by using a two-stage light gas gun at Planetary Exploration Research Center (PERC), Chiba Instiute of Technology, Japan. This gun shoots a projectile with size of 2 mm into a observational chamber filled with gas. The light from the projectile is observed by high-speed camera with 1 Mfps and its spectrum is taken by spectrometer simultaneously.
We carried out a series of experiments using the system with a variety of projectile composition. The specific spectra relating to the projectile component were confirmed as a function of the location from the projectile (during head-neck-tail structure). We will give the experimental results and discuss the chemical and physical status of shooting star.

Keywords: shooting star, impact, spectroscopy

Shock remanent magnetization measurement using the superconducting quantum interference device microscope

*Masahiko Sato[1], Kosuke Kurosawa[2], Masashi Ushioda[1], Sunao Hasegawa[3], Hirokuni Oda[1], Futoshi Takahashi[4], Jun Kawai[5]

1.National Institute of Advanced Industrial Science and Technology, 2.Chiba Institute of Technology, 3.Japan Aerospace Exploration Agency, 4.Kyushu University, 5.Kanazawa Institute of Technology

Knowledge of the evolution of magnetic field intensity is key to understanding the past evolution of planets. However, magnetic field paleointensity data of terrestrial planets such as Mars and Moon have been poorly obtained because of the lack of appropriate rock samples. To address the problem, we focus on shock remanent magnetization (SRM). There are many impact craters on surface of the terrestrial planets, and the magnetic field originated from the SRM of planetary crust can be measured by spacecraft magnetometer. The magnetic field paleointensity could be estimated using the magnetic field data observed over the impact craters.
In order to estimate the magnetic field paleointensity from the observed magnetic field data, it is crucial to know a structure of the SRM, while the structure remains unclear due to the difficulty in experimental techniques. In this study, to reveal the structure of SRM, we conducted SRM acquisition experiments and magnetic imaging of the SRM sample using the superconducting quantum interference device (SQUID) microscope.
Natural basalt samples with cylindrical form of 10 cm in diameter and 10 cm in length (FURNITURE STONE) were used as a target. Before the SRM acquisition experiments, the basalt samples were subjected to alternating field demagnetization at 80 mT. The two-stage light gas gun at the Institute of Space and Astronautical Science (ISAS) of Japan Aerospace and Exploration Agency (JAXA) was used for the SRM acquisition experiments. A magnetically shielded cylinder of 32 cm in diameter and 100 cm in length was set in a vacuum experimental chamber of the two-stage light gas gun. The magnetically shielded cylinder was constructed with three μ-metal layers, and the residual field in the cylinder was <0.3 μT. A solenoid coil of 26 cm in diameter was set in the magnetically shielded cylinder. The basalt sample was placed at the center of the solenoid coil. The applied field was set to be 0–100 μT, and direction of the applied field was parallel to the cylindrical axis of the basalt samples. An aluminum sphere of 2 mm in diameter was used as the projectile. A nylon slit sabot was used to accelerate the projectile. The impact velocity was ~7 km/s, and the impact angle was fixed at 90° from the horizontal.
Using the SQUID microscope at Geological Survey of Japan, National Institute of Advanced Industrial Science and Technology (AIST), magnetic imaging of the basalt samples were conducted after the SRM acquisition experiments. The basalt cylinder was placed on non-magnetic xyz-sample table. The distance between a surface of the basalt cylinder and the SQUID microscope was set to be ~1 cm, and a vertical component of magnetic field over the basalt sample was measured for 6 cm ×6 cm region. The sample imparted SRM in zero-field showed decrease in the magnetic field at center of the crater, corresponding to the increase in sample to sensor distance. On the other hand, the sample imparted SRM in a 100 μT field showed increase in the magnetic field at center of the crater. These results suggest that the basalt samples acquired remanent magnetization as the SRM. In this talk, we will discuss the structure of SRM based on the results of SQUID microscope measurements.

Keywords: Shock remanent magnetization, SQUID microscope

Collisional disruption of meter-sized boulders of the Moon

Kosuke Ando[1], *Tomokatsu Morota[1]

1.Graduate School of Environmental Studies, Nagoya University

The surface condition of planetary bodies reflects its geological evolution. Many boulders are observed on the surface of the Moon. It is thought that collisions of micro bodies disrupt boulders, and makes them fine. Recently, lunar explorations such as SELENE project and Lunar Reconnaissance Orbiter (LRO) obtained high-resolution images of the lunar surface. The high-resolution images allow us to perform statistic investigation of meter scale boulders on the lunar surface.
To reveal the time scale of boulder disruption on the Moon surface and to put constraints on dominant factors (for example, impacter frequency and boulder's strength) for boulder disruption, I performed size-frequency measurement of boulders (D >5 m) on ejecta of 19 small craters (D = 210–920 m), which exist on the floors of Copernicus crater (D = 92.5 km) and King crater (77.3 km). Also, the formation ages of the small craters were estimated from crater densities around the small craters.
The relationship between the boulder frequencies and the formation ages of the small craters indicates that the number densities of boulders decrease exponentially with time. The half-life period of boulder frequency in the King floor is estimated as 75 Myr, about 3 times longer than that in the Copernicus floor. A numerical model of boulder disruption reveals that the impactor frequency and boulder's strength have a significant influence on the survival time of boulders. The observed half-life period of boulders corresponds with a model for size-frequency distribution of impactors with a flatter slope.

Keywords: Moon, boulder, collisional disruption

Relation among the permittivity, density, and volume fraction of crack around craters formed by laboratory impact experiment

*Ken Ishiyama[1], Atsushi Kumamoto[1], Yasuhiko Takagi[2], Norihiro Nakamura[1], Sunao Hasegawa[3]

1.Tohoku University, 2.Aichi Toho University, 3.ISAS/JAXA

The lunar subsurface geological condition was investigated from the measurements of density of core sample [e.g., Carrier et al., 1991] and seismic velocity [e.g., Cooper et al., 1974] in Apollo site. These measurements suggests that the lunar subsurface density decreased with decreasing the depth, which is because there are more impact-induced cracks in the shallow media than in the deep media [e.g., Cooper et al., 1974]. Recently, in order to investigate lunar geological condition, the bulk permittivity of lunar subsurface layer was investigated based on the data from the Lunar Radar Sounder (LRS) onboard the SELENE (KAGUYA) spacecraft [Ishiyama et al., 2013]. Based on the empirical relation among the bulk permittivity, the bulk density, and the porosity, Ishiyama et al. [2013] suggested that the porosity of the lunar subsurface layer was ~19%. However, according to effective medium theory [e.g., Kärkkäinen et al., 2000], the direction of cracks in media can change the relation between the bulk permittivity and bulk density. In this study, we evaluate how the actual crack distribution around impact crater produced in the umpact experiment affect the bulk permittivity, and verify the validity of the estimation method of the porosity and bulk density from the permittivity measured in radar observations.

We performed the impact experiment by using the two-stage light-gas gun at JAXA. First, in order to produce two impact craters, the spherical stainless projectiles with a diameter of 0.32 cm, and mass of 0.133 g at the velocities of ~3.5 and ~5.5 km/s were impacted on two basalt targets with a size of 20 cm×20 cm×10 cm. Next, in order to investigate the influence of anisotropic cracks on permittivity, we drilled two core samples with a diameter of 2.5 cm and length of 8–10 cm along horizontal and perpendicular directions to its impacted surface from basalt target. Finally, we sliced the core sample, and produced sliced sample with a thickness of 3–4 mm. In order to identify the crack distribution on the surface of slice sample, the surface was polished.

In this study, we measured the bulk permittivity, bulk density, and volume fraction of crack of sliced sample. The permittivity of sliced sample was measured at 5 MHz, which is the same with center frequency of the LRS, by using the permittivity measurement system (TOYO Technica Corporation, Type-1260 impedance analyzer and Type-12962A interface). The density of the sliced sample was derived from the measurements of its mass and volume, and the volume fraction of crack of sliced sample was estimated from the ratio of the crack area to the total surface area of the sliced sample. The crack area was identified by applying an image processing to the picture of the surface of the sliced sample.

With the increase of radial distance from crater center, the volume fraction of crack decreased, and the density and permittivity increased. These parameters (i.e., permittivity, density, and volume fraction of crack) strongly depended on the characteristics of the crack distribution around impact crater. In addition, we could confirm difference between the permittivities of sliced samples including the cracks in different directions based on the comparison of slice samples from two core samples along horizontal and perpendicular directions to the surface impacted by the projectile at velocity of ~5.5 km/s. This difference of the permittivity could be explained by the effective medium theory [e.g., Kärkkäinen et al., 2000]. However, since the difference was enough small with respect to the deviation in the measurement of the permittivity of Apollo samples, we could conclude that the estimation method of the porosity and bulk density from the permittivity measured in radar observation was valid.

Experimental investigation on effect of particle size distribution and irregular shape on thermal conductivity of powdered materials

*Naoya Sakatani[1], Kazunori Ogawa[2], Masahiko Arakawa[2], Satoshi Tanaka[1]

1.Institute of Space and Astronautical Science, Japan Aerospace Exploration Agency, 2.Kobe University

Thermal conductivity of regolith on planetary bodies including the Moon and asteroids is one of the most important physical properties for calculating their surface temperature and thermal evolution. We have experimentally investigated the parameter dependences of the thermal conductivity of powdered materials under vacuum conditions mainly using glass beads as a model material. Together with these experimental results, we developed an integrative model for the thermal conductivity, which enable us to estimate the thermal conductivity of powdered materials from the parameter values. However, this model does not explicitly include the effects of particle size distribution and particle shape. Evaluation of their effects on the thermal conductivity is a critical issue to apply our thermal conductivity model to natural regolith on the planetary bodies.
In this study, we measured thermal conductivity of a lunar regolith simulant, JSC-1A, and samples with narrow particle size distributions prepared from JSC-1A by sieve. From these experimental results and our previous experiment data about the glass beads, we evaluated the effects of the wide particle size distribution and irregular particle shape on the thermal conductivity.
Particle sizes of JSC-1A is less than 1 mm, and volumetric median diameter and volumetric arithmetic mean diameter are about 100 μm and 40 μm, respectively. By sieving JSC-1A, we prepared four samples with particle sizes of 53-63 μm, 90-106 μm, 355-500 μm, and 710-1000 μm. We call the sample that is not sieved “JSC-O (Original)” and the samples that are sieved “JSC-S (Sieved)”. Their thermal conductivity was measured by the line heat source method. Degree of vacuum during the measurements was about 0.01 Pa, and ambient temperature was controlled from -25 to 60 ℃. Temperature dependence of the thermal conductivity for each sample was utilized to determine solid conductivity (contribution of the thermal conduction through contact points between the particles) and radiative conductivity (contribution of radiative heat transfer through void spaces between the particle surfaces). The particle size, density, and porosity of the measured samples are summarized in Table 1.
Figure 1 shows experimental results. Because the porosity values of the JSC-S were lower than that of JSC-O (42%) and were scattered from 47% to 66%, we corrected the conductivity to that at the porosity of 42% with using our thermal conductivity model, and these corrected data are also plotted. Moreover, the results for glass beads (porosity of 42%) are also shown.
(1) Effect of particle size distribution: Comparison of JSC-O and JSC-S.
We found that the solid conductivity of JSC-O is comparable with that of JSC-S of 90-106 μm. This particle size is comparable with the volumetric median size of JSC-O. That is to say, it implies that the solid conductivity of a powdered media with a given particle size distribution can be represented as that of a powdered sample with single particle size of the volumetric median. The radaitive conductivity of JSC-O was also comparable with JSC-S 90-106 μm. From these results, we can suggest that the particle size representative of the thermal property is the volumetric median particle diameter.
(2) Effect of particle shape: Comparison of JSC-S and glass beads
The solid conductivity values of JSC-S were comparable with or lower than those of glass beads with the same particle size of each JSC-S. These differences would reflect the difference of the particle shapes, and it is implied that irregular particles have lower solid conductivity than the

spherical particles. On the other hand, we found that the radiative conductivity values of JSC-S and glass beads were comparable. Therefore, we can conclude that the effect of the particle shape on the radiative heat transfer is small, and the radiative conductivity can be modeled with approximation by spherical particles.

Keywords: Regolith, Thermal conductivity

Table 1: Sample list

Sample	Particle size	Density	Porosity
JSC-O	< 1000 μm median 100 μm	1690 kg/m^3	42%
JSC-S	710-1000 μm	980 kg/m^3	66%
	355-500 μm	1110 kg/m^3	62%
	90-106 μm	1460 kg/m^3	50%
	53-63 μm	1540 kg/m^3	47%

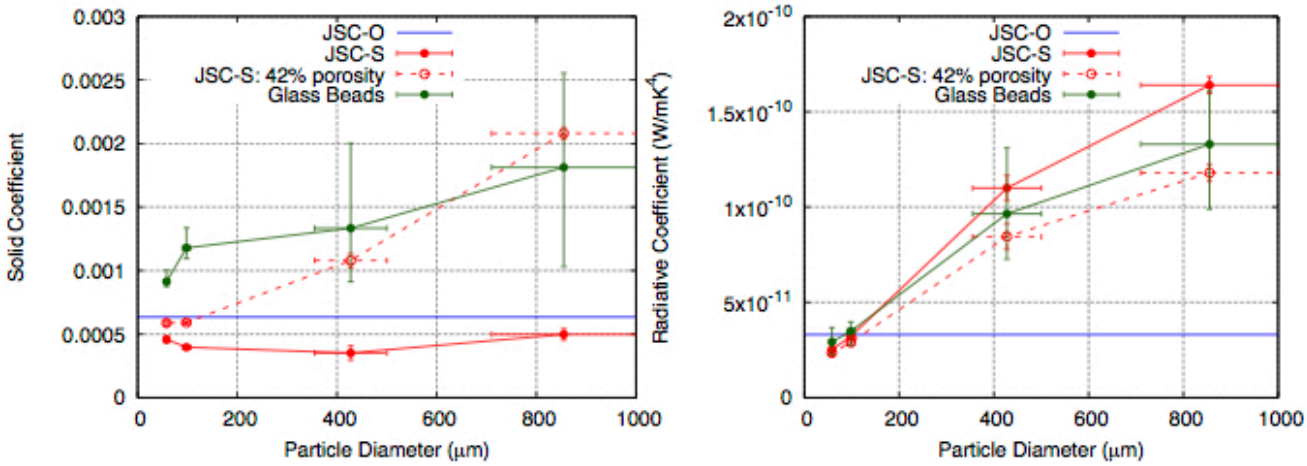

Figure 1: Solid (left) and radiative (right) coefficient of JSC-O (blue), JSC-S (red), and glass beads (green). Dashed red points represent each coefficient that is corrected to porosity of 42%.

Initial operation of Hayabusa2 laser altimeter (LIDAR)

*Hirotomo Noda[1], Takahide Mizuno[2], Noriyuki Namiki[1], Hiroki Senshu[3], Hiroo Kunimori[4], Naoko Ogawa[2], Hiroshi Takeuchi[2], Makoto Shizugami[1]

1.National Astronomical Observatory of Japan, 2.Japan Aerospace Exploration Agency, 3.Chiba Institute of Technology, 4.National Institute of Information and Communications Technology

The Hayabusa2 asteroid explorer was launched on December 3,2014. The spacecraft orbited around the Sun for a year, and after an Earth Gravity Assist operation, the spacecraft was inserted into a transfer orbit to the target asteroid 162173 Ryugu for the arrival at 2018. The first checkout of a laser altimeter called LIDAR onboard Hayabusa2 was done on January 23, 2015, and a rehearsal operation for the coming laser link experiment was done on August 27, 2015, and the laser link experiments had been done between October and December 2015. In this paper, we will discuss the following three issues of the LIDAR based on the result of the initial operation.i) Estimation of the boresight direction of the receiving telescope: We conducted an experiment in which laser pulses were transmitted toward the LIDAR from ground-based satellite laser ranging stations and the LIDAR bounced the laser toward the Earth. We call the experiment as laser link experiment. In this experiment, we set the observational mode as “optical transponder” mode. As the boresight direction was not determined well at first, the attitude of the spacecraft was scanned spirally outward from a center with 1 mrad separation, and the direction of the boresight of the receiving telescope was estimated when the LIDAR detected the laser pulses from the ground. Based on results of three days experiment, we found out that the boresight direction was closer with 0.2 degrees to the -Z axis of the spacecraft compared with what was measured before the launch with alignment cubes. However, the estimated boresight directions differs about 1 mrad for each day. So far we do not have any good reasons for that. Therefore, we concluded that the boresight was determined with the ambiguity of 1 mrad, and it must be updated after arriving at the target asteroid by detecting notable topographic features. The alignment between the transmitting and the receiving telescope has not been confirmed yet, because we have not detected the downlink laser pulses from the LIDAR on the ground station.ii) Confirmation of the ranging function: In the normal ranging, a gate is set just after the laser is transmitted to inhibit the detection of the laser. As a checkout of the instrument, however, we did not set the gate so that the scattered stray light can be detected to make the ranging circuit operated. We call this operation “non-gate ranging”. During the initial checkout, we conducted the non-gate ranging for three times, on January 23,August 27, and December 16. We confirmed that the ranging circuit worked without any problem on each day. The value of the pseudo range (the time between transmission and reception of the laser) did not show any change for each day. The averaged laser power was also confirmed normal, taking into account the deviation from the averaged value. The reception power changed in accordance with the transmission energy. Considering all these evidences, we concluded that the ranging function was normal.iii) Evaluation of the reception noise level: In both ranging mode and optical transponder mode, we observed such phenomenon that the detection flags became ON thought the reception power showed zero, and that the frequency of this phenomenon increased as the smaller threshold level of the reception was set. Assuming that this was because of the noise from the AD converter, we conducted a test operation on August 27 to clarify the boundary in which the frequency increased. As a result, we found that the threshold level at which noise increased as between 12 mV and 14 mV. In the ranging mode, the recommended threshold level is 27 mV or 45 mV, therefore practically the influence of the noises will be insignificant. However, in the “dust counting mode” which aims to detect the levitation dust near the asteroid, the threshold will be set comparable or lower than this value, because the

detection level estimated from the dust flux is expected to be low.

Keywords: Hayabusa2, asteroid, laser altimeter

JUICE/GALA-J (1) : The Ganymede Laser Altimeter (GALA) for the JUICE mission - Introduction, current status, and role of the Japan team

*Keigo Enya[1], Noriyuki Namiki[2], Masanori Kobayashi[3], Jun Kimura[4], Hiroshi Araki[2], Hirotomo Noda[2], Shoko Oshigami[2], Shingo Kashima[2], Ko Ishibashi[3], Shingo Kobayashi[5], Masanobu Ozaki[1], Takahide Mizuno[1], Shin Utsunomiya[1], Yoshifumi Saito[1], Kazuyuki Touhara[1], Shunichi Kamata[5], Koji Matsumoto[2], Kiyoshi Kuramoto[5], Sho Sasaki[6], Satoru Iwamura[7], Teruhito Iida[8], Yoshiaki Matsumoto[8], Masanori Fujii[9], Naofumi Fujishiro[10], Tomoyasu Yamamuro[11], Kay Lingenauber[12], Thomas Behnke[12], Juergen Oberst[12], Judit Jaenchen[12], Horst-Georg Loetzke[12], Harald Michaelis[12], Hauke Hussmann[12]

1.JAXA/ISAS, 2.NAOJ, 3.CIT, 4.Earth-Life Science Institute, Tokyo Institute of Technology, 5.Hokkaido University, 6.Osaka University, 7.MRJ, 8.PLANET, 9.FAM Science, 10.Astro-Opt, 11.OptCraft, 12.DLR

We present an introduction, current status, and especially role of the Japan team for the Ganymede Laser Altimeter (GALA) for the Jupiter Icy Moon Explorer (JUICE) mission. JUICE is a mission of ESA to be launched in 2022, and GALA is one of the payloads of JUICE.
Major objectives of GALA are to provide topographic data of Ganymede, the largest satellite of Jupiter, and to measure its tidal amplitudes. The latter is crucially important to detect and to characterize an underground ocean on Ganymede. Furthermore, GALA support geological studies, e.g., identification of characterization of tectonic and cryo-volcanic regions, impact basins, and craters. GALA also provides information on surface roughness and the albedo.
For the laser altimetry, GALA emits and receives laser pulses at about 500 km altitude above Ganymede. Wavelength, energy, and nominal repetition frequency of the laser pulse are 1064 nm, 17 mJ, and 30 Hz, respectively. Reflected beam from the Ganymede surface is received by the receiver telescope with 25 cm diameter aperture, re-focused by the BEO including a narrow band-pass filter, and then detected by the APD detector.
Development of GALA is carried out in international collaboration from Germany, Japan, Switzerland, and Spain. GALA-Japan will develop the Backend Optics (BEO), the Focal Plane assembly (FPA) including an avalanche photo-diode (APD) detector, and the Analog Electronics module (AEM) in the receiver chain. It should be noted that responsibility of development of the receiver telescope has been moved from Japan to Germany. Based on the heritage of studies for the telescope, GALA-Japan will contribute to the receiver telescope development through the German team.

Keywords: JUICE, GALA, Jupiter, Icy moon, Ganymede, Laser altimeter

Orbital and tidal evolution of Enceladus

*Ayano Nakajima[1], Shigeru Ida[1], Jun Kimura[2]

1.Department of Earth and Planetary Sciences, Tokyo Institute of Technology, 2.Earth-Life Science Institute, Tokyo Institute of Technology

Among Saturn's mid-sized moons, only Enceladus is thermally active, which has been a big puzzle. We have performed numerical simulations of tidal orbital evolution of the Saturn's mid-sized moons and evaluated tidal heating in Enceladus.
The current heat flux of Enceladus was estimated as ~16 GW by Cassini's observation (Howett et al. 2011). If the time-averaged dissipation factor Q of Saturn is anticipated as ~18000, the heat production is estimated to be 1.1 GW (Meyer & Wisdom 2011), which is much smaller than the observed value. Recently, a smaller value of Q_{Saturn} (~1680) was suggested by astrometric data analysis (Lainey et al. 2010). If Q_{Saturn}=1680, the mid-sized satellite may have formed from the ring (Charnoz et al. 2011). In this model, Enceladus must be formed earlier than Tethys and their orbits must closely approach each other in the course of tidal orbital evolution.
Through numerical orbital integration taking into account tidal interactions, we found that Enceladus is captured at a mean-motion resonance with Tethys. Because Tethys is more massive and accordingly its orbital evolution is faster, Enceladus' semi-major axis is pushed by Tethys and its eccentricity is secularly increased until its orbit starts crossing with Tethys' orbit. Eventually, Enceladus is scattered inward and Enceladus and Tethys establish the current orbital order. After the inward scattering, Enceladus becomes isolated from Tethys and its large eccentricity is damped by tidal dissipation inside Enceladus. The heat generation may be large enough to account for the current heat flux. Because this process occurs only for Enceladus, it can explain why only Enceladus is thermally active.

Keywords: Enceladus, tidal heating, orbital evolution, mean motion resonance

Interior thermal state of Enceladus: an inference from the relaxation state of its icy shell

*Shunichi Kamata[1], Francis Nimmo[2]

1.Creative Research Institution, Hokkaido University, 2.UC Santa Cruz

The South Polar Terrain of the icy Saturnian satellite, Enceladus, is one of the most geologically active regions among icy worlds. The origin of the anomalously large amount of heat observed over this region by the Cassini spacecraft is still unclear. To understand the heat budget of Enceladus, the interior thermal state should be investigated. This study attempts to constrain the thermal structure of Enceladus by comparing two timescales: those for viscous relaxation and melting. The subsurface ocean underneath the South Polar Terrain is thicker than other areas; the crust is thin in this region. Such “topography” at the base of the shell should viscously relax over time, and its timescale depends on the temperature of the deep part of the shell. If the shell is hot and has a low viscosity, the relaxation timescale should be short; a regionally thickened subsurface ocean cannot be maintained.On the other hand, if the laterally flowing portion of the shell melts, then a regionally thickened subsurface ocean can be maintained. In this study, we conduct numerical calculations of viscoelastic deformation under a wide variety of parameter conditions and compare timescales of viscoelastic relaxation and melting of the shell. Our results indicate that the former timescale is much shorter than the latter if we consider conventional values for radiogenic heating (0.3 GW [Roberts & Nimmo, 2008]) and tidal heating (1.1 GW [Meyer & Wisdom, 2007]). Our results also indicate that >10 GW, about one order of magnitude larger than the conventional value, is necessary to make those timescales comparable. This result suggests that the current Enceladus is unlikely to be in a steady-state; previous episodic heat production may contribute significantly to the current thermal state of Enceladus.

Keywords: Enceladus, Icy satellite, Viscoelastic

Numerical experiments on mantle convection of super-Earths with variable thermal conductivity and adiabatic compression

*Masanori Kameyama[1], Mayumi Yamamoto[1]

1.Geodynamics Research Center, Ehime University

We conduct a series of numerical experiments of thermal convection of highly compressible fluid in a two-dimensional rectangular box, in order to elucidate the mantle convection on super-Earths. The thermal conductivity and viscosity are assumed to exponentially depend on depth and temperature, respectively, while the variations in thermodynamic properties (thermal expansivity and reference density) with depth are taken to be relevant for the super-Earths with 10 times the Earth's. Our experiments showed the change in convecting flow patterns depending on the depth-dependence in thermal conductivity and the temperature-dependence in viscosity. This is largely due to the change in the thermal state in the convecting mantle, whose interplay with the adiabatic temperature change in turn reduces the activity of hot plumes from the base of the mantle. In particular, for the cases with strong interplay, we found that a "deep stratosphere" of stable thermal stratification can form at the base of the mantle where the fluid motion is insignificant. We also found that the presence of "deep stratosphere" not reduces but enhances the overall heat transport through the mantle, although it weakens the vigor of mantle convection. Our finding may further imply that the absence of intrinsic magnetic fields on massive terrestrial planets is not a corollary of the lack of plate tectonics on their surfaces.

Keywords: super-Earths, mantle convection, adiabatic (de)compression

High dimensional coupled spin model for polarity reversals

*Ariyoshi Kunitomo[1], Akika Nakamichi[2], Tetsuya Hara[1]

1.Kyoto Sangyo University, 2.Koyama Astronomical Observatory, Kyoto Sangyo University

Recently, the macro spin model has been suggested for polarity reversal (Nakamichi et al. 2012, Mori et al. 2013). This is the idea that geomagnetism is described by interaction with many local dynamo elements (called macro-spins). This model can reproduce many features of geomagnetism and the solar magnetism; power spectrum, average time of polarity flipping, randomness and periodicity of polarity reversals.We study this model to become higher dimensional model. In this result, our model becomes possible for many things which are not treated in previous study, for example reproduce migration of the North (or South) Magnetic Pole, comparison with observed data of magnetic field distributions expressed in two directions.In addition, we investigate some distribution function that the pole migration followed and make a comparison with previous study, e.g. Lévy distribution (Carbone et al., 2006) and log-normal distribution (Ryan & Sarson, 2007).

Keywords: geomagnetism, solar magnetism, coupled-spin

Development of Exoplanet database “ExoKyoto” aiming for inter-comparison with different criteria of Habitable zones

Yosuke Yamashiki[1], Takaaki Ito[3], Yuji Shimada[3], Mariko Inazawa[4], *Takanori Sasaki[2], Osamu Nishiura[4], Shota Notsu[2], Hiroyuki Ishikawa[5], Anna Suzuki[6], Takahito Sakaue[5], Yuuta Notsu[2], Naoki Nakamura[2], Kosuke Namekata[5], Hiroaki Isobe[1], Kazunari Shibata[2], Saaya Shimozaki[7], Shione Fujita[7]

1.Graduate School of Advanced Integrated Studies in Human Survivability Kyoto University, 2.Graduate School of Science, Kyoto University, 3.Faculty of Agriculture, Kyoto University, 4.Faculty of Engineering, Kyoto University, 5.Faculty of Science, Kyoto University, 6.Graduate School of Science, Kyoto Sangyo University, 7.SGH Shiga Prefectural Moriyama High School

An integrated database of confirmed exoplanets, capable in comparing several different definition of Habitable Zone, is developed and launched as “ExoKyoto”, for the purpose of better comprehension of those existing celestial entities in different star system. The ExoKyoto core-module is written in C++ with definition of different classes as “ExoPlanet” and “HostStar” objects. The classification of Habitable zone for each host star is based on Kopparapu et al. (2013) as the reference cases, at the same time this database determine Solar Equivalent Astronomical Unit (SEAU) to promote easy comprehension of different star system equivalent to that of Solar System.
The database has inter-comparison module with existing exoplanet database as Exoplanet.eu, Open Exoplanet Catalogue, and NASA exoplanet archive, and updating module in order to secure commonly agreed value for each planet. Since most of exoplanets found by Kepler spacetelescope detected only by transit method does not confirmed their mass by radial velocity, a mass estimation module for most of Super-Earth sized planets is included developed based on the Larsen and Geoffrey (2014). Using this mass-assumption module, the portion of Super-Earth sized exoplanets (2-10 Mearth) become dominant (794 among 1988) compared with that of super jovian sized ones (>500 Mearth) (480 among 1988), being comparable to total jovian & super jovian planets (926), in which only 140 of those Super-Earth sized mass has confirmed by radial velocity. Throughout the comparison between habitable criteria by Kopparapu et al. (2013) and ours (SEAU), most of exoplanets orbiting around M type stars have different conditions each other. The potential impact of stellar flares on those exoplanets can be discussed using our database.
For outreach purpose, ExoKyoto possesses interface with GoogleSky for easy comprehension of those celestial bodies among stellar map.
Lauren M. W. and Geoffrey W. M. 2014. The mass-radius relation for 65 exoplanets smaller than 4 earth radii. *The Astrophysical Journal Letters*, 783:L6
Kopparapu R. K. et al. 2013. Habitable Zones Around Main-Sequence Stars: New Estimates. *The Astrophysical Journal*, 765:131

Keywords: Exoplanet, Habitable Zone, SEAU

observation and analysis of exoplanets by using Dipol-2 of T60 telescope at Haleakara mountain

*Haruaki Maeda[1], Takeshi Sakanoi[1], Masato Kagitani[1]

1.Planetary Plasma and Atmospheric Research Center, Graduate School of Science, Tohoku University

We have started continuous observation of exoplanets from January 2015 by a method of polarimetry using DIPOL-2 (a double image high precision polarimeter, Piirola_et., al 2014) attached to Haleakara T60 telescope. The light scattered or reflected in the planetary atmosphere is linearly polarized. An observer receives the polarized light from the exoplanet as well as non-polarized light from a main star. Thus, periodic variation of linear polarization is observed as the exoplanet orbits around the main star. The polarimetry gives us an information about orbital elements of the exoplanet as well as their atmosphere, even if they do not transit the main stars. Practically, maximum degree of polarization is about an order of -4 through -5 for typical hot Jupiter. Because of difficulties of such a high-precision polarimetry, there is only a successful polarimetry of exoplanet (Berdyugina et al., 2008 2011). One of the primal goal of this study is to establish an observing technique and a analysis method for high-precision polarimetry. To achieve high-precision polarimetry better than 10^(-5), , we need to determine instrumental polarization carefully. First, we analyzed measurements of two high-polarized star (HD204827,HD25443) which enable us to determine reference axis of linear polarization. Then we made analysis of non-polarized standard stars to determine the instrumental polarization. In 2015, we have observed non-polarized standard stars 19 in January, 12 in May, 18 in Augustand 10 in October, 59 in total.. Then, we derived instrumental polarization at accuracy of 10^(-5), except for the data in January which do not have enough tracking accuracy. We also have several measurement of three exoplanets (tau_boo b, HD189733 b, 55Cnc e). We would be able to get variation of polarization of exoplanets by subtracting instrumental polarization from the observed polarization. We chose hot Jupiter type exoplanets as observing targets, because they rotate around the main stars by two or three days and we can get polarimetric measurements in the different phase angle within a short time. In this presentation, we will present the recent result of instrumental polarization, method of estimation of the exoplanets' polarization and the recent result from the three exoplanets.

Keywords: exoplanet, polarization, observation, atmosphere, scaterring

UV space telescope for exoplanetary systems

*Hiroki Horikoshi[1], Shingo Kameda[2], Go Murakami[3], Masahiro Ikoma[4], Norio Narita[5]

1.Graduate School of Science, Rikkyo University, 2.School of Science, Rikkyo University, 3.Institute of Space and Astronautical Science, Japan Aerospace Exploration Agency, 4.Department of Earth and Planetary Science, Graduate School of Science, The University of Tokyo, 5.National Astronomical Observatory of Japan

Many observations have been carried out for exoplanets since they were first discovered in 1995. To date, the number of detected exoplanets is more than 1900. Some of them are known about their atmospheric composition.
Compared the Earth with the planets which exist in solar system, the Earth has much more oxygen which is produced by photosynthesis. Therefore, detection of oxygen on planets is one of the key factors to characterize exoplanets. In this work, we aim to detect O I emission (130.6 nm) in planet atmospheres by using UV space telescope.
Because planets orbit around its parent star, light of planets whose wavelength is slightly changed with Doppler shift is observed. Therefore, if Doppler shift is large and the parent star's continuum doesn't exist, emissions of planets can be separated from light of its parent star by using high dispersion spectrometer. Because the habitable zones of low-temperature stars are near the parent star, if an Earth-like planet exists in the habitable zone of a low-temperature star, the orbital velocity is fast and the Doppler shift is large. In this work, we assume that the Earth exists in the habitable zones of low temperature star. Then, planetary O I emission can be separated from its parent star. However, because its intensity is very weak, we need to use a large and high efficiency telescope, which exceeds Hubble Space Telescope.
NASA and ESA are planning to launch space telescope dedicated to exoplanets; however, their spectral ranges are limited to the visible and infrared regions. Therefore, we are planning to develop a UV space telescope dedicated to exoplanetary systems. In this presentation, we introduce the study situation and specification of instruments.

Keywords: exoplanet, ultraviolet, space telescope

BepiColombo Euro-Japan Joint mission to Mercury

*Hajime Hayakawa[1], Hironori Maejima[1]

1.The Institute of Space and Astronautical Science/Japan Aerospace Exploration Agency

BepiColombo is a ESA-JAXA joint mission to Mercury with the aim to understand the process of planetary formation and evolution in the hottest part of the proto-planetary nebula as well as to understand similarities and differences between the magnetospheres of Mercury and Earth.
The baseline mission consists of two spacecraft, i.e. the Mercury Planetary Orbiter (MPO) and the Mercury Magnetospheric Orbiter (MMO). JAXA is responsible for the development and operation of MMO, while ESA is responsible for the development and operation of MPO as well as the launch, transport, and the insertion of two spacecraft into their dedicated orbits.
MMO is designed as a spin-stabilized spacecraft to be placed in a 600 km x 11400 km polar orbit. The spacecraft will accommodate instruments mostly dedicated to the study of the magnetic field, waves, and particles near Mercury. While MPO is designed as a 3-axis stabilized spacecraft to be placed in a 400km x 1500 km polar orbit. Both spacecraft will be in same orbital plane.
Critical Design Review(CDR) for MMO project is completed in November 2011 while ESA Spacecraft CDR is completed in Novemver 2013. MMO stand alone FM AIV is completed on March 2015. MMO FM was transported to ESA/ESTEC on April. Stand alone activity for MMO was completed in December 2015. MMO is waiting for the stack level (MCS) final AIV. BepiColombo is expected to be launched in 2017.
BepiColombo science working team (SWT) meeting, which discusses science related matters, was held once a year and will be held twice a year from this year. In this paper, BepiColombo project as a test case of large collaboration between ESA and JAXA will be reported.

Keywords: Mercury, Planetary Exploration, International Collaboration

JUICE/GALA-J (2): Science objectives of the GAnymede Laser Altimeter (GALA) for the JUICE mission

*Jun Kimura[1], Shunichi Kamata[5], Koji Matsumoto[2], Shoko Oshigami[2], Noriyuki Namiki[2], Kiyoshi Kuramoto[5], Sho Sasaki[8], Keigo Enya[4], Masanori Kobayashi[3], Shingo Kobayashi[6], Hiroshi Araki[2], Hirotomo Noda[2], Ko Ishibashi[3], Yoshifumi Saito[4], Hauke Hussmann[7], Kay Lingenauber[7]

1.Earth-Life Science Institute, Tokyo Institute of Technology, 2.National Astronolocal Observatory Japan, 3.Chiba Institute of Technology, 4.ISAS/JAXA, 5.Hokkaido University, 6.National Institute of Radiological Sciences, 7.German Aerospace Center, 8.Osaka University

The JUpiter Icy Moons Explorer (JUICE), led by European Space Agency, has started development toward launch in 2022 (arrival at Jupiter in 2029, and Ganymede orbit insertion in 2032), and we are now developing the GALA instrument onboard JUICE spacecraft collaborating with German Aerospace Center (DLR) and other institutions in Europe. Primary objective of GALA is to acquire the key information for understanding the evolution of icy bodies and to play an essential role in the JUICE's purpose: exploration of deep habitat.
Jovian icy moon Ganymede, which is the largest moon in the Solar System and the primary target of the JUICE, can be said to be one of the typical solid bodies along with terrestrial planets in terms of its size and the intrinsic magnetic field originated from the metallic core. However, current knowledge provided by previous explorations is extremely limited since it comes from only several fly-bys. The JUICE will uncover the whole picture of Ganymede by the first "orbiting" in the history around extra-terrestrial moon. Expected new big picture of the origin and evolution of Ganymede will not only be a key to unveil the origin of diversity among the Solar System bodies, but also contribute to understand exoplanets with a wide diversity.
The GALA will measure a distance between the spacecraft and the surface of icy moons and acquire the topography data (globally for Ganymede, and fly-by region for Europa and Callisto). It will be a first-ever laser altimetry for the icy object. Such information makes surface geologies clear and tremendously improves our understanding of the icy tectonics. By comparing their tectonic styles on the rocky planets/moons, GALA data leads to reconsider the Earth's plate tectonics. In addition, the GALA will confirm a presence/absence of the subsurface ocean by measuring tidal and rotational response, and also the gravitational information reflecting the interior structure will be greatly improved. In addition, strength and waveform of laser pulse reflected from the moon's surface have information about surface reflectance at the laser wavelength and small scale roughness, and therefore we can see degrees of erosion and space weathering without being affected by illumination condition through GALA measurements.
In order to interpret and understand such measurements, accumulated studies for the Earth over the years will be effectively utilized: e.g., the data for surface topography, roughness and albedo will lead to describe the icy tectonics through the knowledge from terrestrial glaciology and experiments on impact and deformation process. The tidal measurements by GALA will also be a window to see its interior based on our knowledge and experiences cultivated through the past geodetic observations, e.g., the SELENE mission for the terrestrial Moon.
Characterization of the icy moons will be achieved not only from the GALA measurements but also synergy of other scientific instruments onboard JUICE spacecraft, for examples, surface images taken by optical camera (JANUS) will confirm the position of GALA laser footprint to complement the GALA "point" data for precise topographic mapping. A radar sounder (RIME) and a radio science experiment (3GM) probe the interior structure, especially interior of the icy crust to figure out an occurrence of tectonic features. A visible and infrared imaging spectrometer (MAJIS), an

ultraviolet imaging spectrograph (UVS) and a sub-millimeter wave instrument (SWI) will acquire a surface and atmosphere compositional data. A magnetometer (J-MAG) monitors moons' inductive response to the Jovian magnetic field and probes the subsurface ocean with the help of a particle environment package (PEP) and a radio and plasma wave investigation (RPWI). The GALA works closely together with these instruments and plays a leading and a supporting role to clarify the whole picture of Ganymede and other icy moons.

JUICE/GALA-J (3): Performance model simulation of Ganymede Laser Altimeter (GALA) for the JUICE mission

*Hiroshi Araki[1], Noriyuki Namiki[1], Hirotomo Noda[1], Ko Ishibashi[2], Keigo Enya[3], Masanobu Ozaki[3], Takahide Mizuno[3], Shin Utsunomiya[3], Yoshifumi Saito[3], Kazuyuki Touhara[3], Shoko Oshigami[1], Shingo Kashima[1], Jun Kimura[4], Shingo Kobayashi[5], Masanori Kobayashi[2], Gregor Steinbruegge[6], Alexander Stark[6], Christian Althaus [6], Simone DelTogno[6], Kay Lingenauber[6], Hauke Hussmann[6]

1.National Astronomical Observatory of Japan, 2.Planetary Exploration Research Center, Chiba Institute of Technology , 3.Institute of Space and Astronautical Science, Japan Aerospace Exploration Agency, 4.Earth-Life Science Institute, Tokyo Institute of Technology, 5.National Institute of Radiological Sciences, 6.Deutsches Zentrum für Luft- und Raumfahrt

The laser altimeter GALA (GAnymede Laser Altimeter) is one of the payload instrument of JUICE (JUpiter ICy moons Explorer) project led by ESA to be launched in 2022. GALA is developed by the international collaboration by Germany, Japan, Switzerland, and Spanish teams.

In order to clarify the requirement on the interface conditions between modules of GALA, we developed the performance model of GALA based on the model of BELA (Bepi-Colombo Laser Altimeter). The performance model quantifies the link budget, range accuracy, albedo measurement accuracy, and probability of false detection (PFD). In the performance model, background noise from scattered sunlight from the Ganymede surface, surface and bulk dark currents of APD, noise floor of APD-TIA, shot noise, and speckle noise are taken into consideration. Black-body emission from the Ganymede surface is also taken into account while its influence to SNR is negligible compared with other noises. EMI noise shall be included after the evaluation of the verification model.

Scientific requirements on GALA performance is summarized into the following four criteria: [1] For Europa fly-by, PFD is less than 0.2 from an altitude of 1300 km or lower, [2] Under the worst observation condition for albedo and surface slope of GCO500 (Ganymede Circular Orbit whose height is 500km), the accuracy of the ranging is less than 10 m and PFD is less than 0.2. [3] Under the nominal observation condition of GCO500, the accuracy of the ranging is less than 2 m and PFD is less than 0.1. [4] Under the best observation condition of GCO500, the accuracy of the ranging is less than 1 m and PFD is less than 0.1.

Returned laser pulse is converted to analogue signal in Japanese Analogue Electric Module (AEM), then to digital signal and transferred to Swiss Range Finder Module (RFM). RFM applies matched filtering to the digital signal to determine the range as accurately as possible. The signal processing in RFM constrains the performance of AEM, therefore, GALA-J developed its own matched filter simulation aiming to determine the signal-to-noise ratio (SNR). The matched filtering in RFM is a convolution of signal and Gaussian filter whose width in time domain is adjustable. The filtering is thus equivalent to moving average weighted by Gaussian filter in time domain. In this simulation, the length of range gate is 8192 and the sampling frequency is 66.7 MHz which is lower than the current design of ADC of 200 MHz. The band-pass filtering by trans-impedance amplifier of APD (APD-TIA) is taken into account by filtering the return pulse and APD noise by 100 MHz. By changing input SNR and width of the Gaussian filter, the lower bounds of the output SNR that satisfy the system requirements are investigated. The requirements for the input SNR obtained by the investigation are then confirmed well below the analogue SNRs calculated by the performance model.

The return signal is assumed to have a Gaussian form in both spatial and time domain in this performance model, however, the broadening occurs on a reflection by the surface topographic roughness and filtering processes in AEM and RFM. These effects on the results are now investigated and will be shown at the poster presentation.

Keywords: Jupiter, Ganymede, JUICE, GALA, Laser altimeter, Performance model

JUICE/GALA-J (4): Electronics and detector development for Ganymede Laser Altimeter (GALA) for the JUICE mission

*Masanori Kobayashi[1], Osamu Okudaira[1], Ko Ishibashi[1], Masayuki Fujii[6], Keigo Enya[2], Noriyuki Namiki[3], Hiroshi Araki[3], Hirotomo Noda[3], Shoko Oshigami[3], Shingo Kashima[3], Masanobu Ozaki[2], Takahide Mizuno[2], Shin Utsunomiya[2], Yoshifumi Saito[2], Kazuyuki Touhara[2], Jun Kimura[4], Shingo Kobayashi[5], Hauke Hussmann[7], Kay Lingenauber[7], Thomas Behnke[7], Simone DelTogno[7]

1.Planetary Exploration Research Center, Chiba Institute of Technology, 2.Institute of Space and Astronautical Science, Japan Aerospace Exploration Agency, 3.National Astronomical Observatory of Japan, 4.Earth-Life Science Institute, Tokyo Institute of Technology, 6.National Institute of Radiological Sciences, 5.National Institute of Radiological Sciences, 6.FAM Science Co., LTD., 7.Deutsches Zentrum für Luft- und Raumfahrt

Ganymede Laser Altimeter (GALA) is scheduled on board JUICE mission by ESA to be launched in 2022. GALA will be developed and manufactured jointly by teams of Germany, Japan, Switzerland, and Spain. Japanese team is responsible for subunits of a receiver unit out of GALA instrument; a backend optics (BEO), a focal plane assembly (FPA) accommodating an APD sensor module and an analog electronic module (AEM). In our poster presentation, the current development status of APD module and AEM of GALA will be reported.
The APD sensor is mounted on a hybrid IC of the APD module including a trans-impedance amplifier (TIA) for signal readout in a wide band width as 100MHz, a thermo-sensor for measurement of the APD sensor temperature and a thermoelectric (TE) cooler for control of the APD sensor temperature to stabilize the temperature as 25 deg-C or so. The APD sensor has an enhanced quantum efficiency of up to 40% at 1060 nm. APD typically has a large temperature dependency of gain. The APD module is equipped with TE cooler and the TE cooler is capable to control the temperature of APD precisely.
The TIA in the APD module outputs voltage signals corresponding to the input light pulses. The voltage signals are fed into the AEM. The transmitted pulses introduced from LHM are attained not to overshoot by a programmable amplifier in the AEM because the following part of analogue signal processing circuit in AEM is to be tuned for signals returned from the target body which are much smaller than the introduced laser pulses. Signal waveform from the introduced laser pulse to the received return pulse is converted to digital data by analogue-to-digital conversion (ADC) circuit and digitized waveform are transmitted to a range finder module (RFM).
As of writing this abstract, we are preparing radiation test campaign of APD to evaluate and qualify the APD sensor of the module and also building a bread board model of AEM to evaluate development challenges in that.

Keywords: JUICE, GALA, APD, Ganymede, Laser Altimeter

JUICE/GALA-J (5): Radiation analysis for Ganymede Laser Altimeter (GALA) for the JUICE mission

*Shingo Kobayashi[1], Simone DelTogno[2], Masanori Kobayashi[3], Masanobu Ozaki[4], Keigo Enya[4], Takahide Mizuno[4], Makoto Utsunomiya[4], Yoshifumi Saito[4], Kazuyuki Touhara[4], Ko Ishibashi[3], Noriyuki Namiki[5], Hiroshi Araki[5], Hirotomo Noda[5], Shoko Oshigami[5], Shingo Kashima[5], Jun Kimura[6], Christian Althaus[2], Kay Lingenauber[2], Hauke Hussmann[2]

1.National Institute of Radiological Sciences, 2.Deutsches Zentrum für Luft- und Raumfahrt, 3.Planetary Exploration Research Center, Chiba Institute of Technology, 4.Japan Aerospace Exploration Agency, 5.National Astronomical Observatory of Japan, 6.Earth-Life Science Institute, Tokyo Institute of Technology

The radiation environment around the Jupiter consists of electrons and protons that are trapped by the Jupiter's magnetosphere, solar energetic particles and galactic cosmic-rays. The trapped electrons are the most harmful to devices on the JUICE because the trapped electron flux is the most intense and the its penetrability is relatively higher than the other charged particles. The solar energetic particles are of secondary importance in spite of the lower flux because its energy spectrum is hard and the high energy protons easily penetrate a shield.
The most sensitive device to radiation on the GALA is the avalanche photo diode (APD) to detect the laser pulses returned from the Ganymede's surface. The maximum tolerance, total ionizing dose (TID), is relatively lower than the other devices and is 30 krad. Thus, an adequate shielding is required to reduce the degradation of the performance of the APD. In order to estimate the radiation dose at the APD, a simulation application, GALA-sim and GALA-analy, based on Geant4 [1] and ROOT [2] was developed by GALA Japan to estimate the radiation dose during Jupiter cruising. The application can import for a radiation analysis a three dimensional CAD model which is produced as a result of our structural and strength design of the GALA instrument. It also can estimate the influence of secondary neutron production by nuclear reactions in JUICE in addition to the primary trapped electrons and the solar energetic particles.
The preliminary three dimensional model of the GALA Transceiver Unit (TRU), GAL-TRU-i1.4-Shielding, was developed to analyze the radiation dose during the JUICE mission. The average thickness of mass around the APD in this model is 11.4 g/cm^2 which corresponds to aluminum which 42 mm thickness. The TRU was irradiated with trapped electrons and solar energetic particles by the GALA-sim based on Geant4 version 9.6.p03 and 10.01.p01 and TIDs at the APD due to trapped electrons and solar energetic particles were estimated. They are 21.2 and 0.72 krad (Figure of safety, FoS=2), respectively, if calculated by Geant4.10.01. The sum of TIDs fell below the maximum tolerance of the APD (30 krad). The radiation dose due to the trapped electrons is 30 times higher than that of solar energetic particles as expected. It is found that the trapped electrons with an energy of 10-40 MeV mainly contributes the TID. No dependency on the versions of Geant4 was observed and both results are consistent each other within 3% difference. The result was also confirmed by the calculation by FASTRAD [3].
The total non-ionizing dose (TNID) which is the energy deposition on a material via non-ionizing processes such as Coulomb scattering, nuclear elastic scattering and nuclear reactions, and results in displacement damage is also estimated based on the theory of non-ionization energy loss by [4] with the help of GRAS [5]. The TNID due to the primary trapped electrons, the primary solar protons and the secondary neutron at the APD is 7.52x10^{7}MeV/g (FoS=2) which is equivalent to the 50 MeV proton flux of 1.75x10^{10} cm^{-2}. The contributions of each particles to TNID were 71%, 24% and 5%, respectively.

In summary, we have developed a simulation code to estimate the radiation damage of the devices in GALA instrument. We found the reasonable solution for the radiation shielding of the APD. The results of calculation are used for the radiation test of the APD at a beam irradiation facility and the improvement of the design of TRU.

[1] S. Agostinelli et al., Nucl. Instr. and Meth. A506 (2003) 250-303.
[2] R. Brun and F. Rademakers, Nucl. Inst. & Meth. A389 (1997) 81-86.
[3] TRAD, http://www.fastrad.net/
[4] I. Jun et al., IEEE Trans. Nucl. Sci., 50 (2003) 1924-1928.
[5] G. Santin et al., IEEE Trans. Nucl. Sci. 52 (2005) 2294-2299.

Keywords: Jupiter, Ganymede, JUICE, GALA, Laser altimeter, radiation analysis

JUICE/GALA-J (6): Optical/thermal/structural design for the receiver part of the Ganymede Laser Altimeter (GALA) for the JUICE mission

*Keigo Enya[1], Masanori Kobayashi[2], Ko Ishibashi[2], Shingo Kashima[3], Shin Utsunomiya[1], Satoru Iwamura[4], Teruhito Iida[5], Yoshiaki Matsumoto[5], Masanori Fujii[6], Naofumi Fujishiro[7], Tomoyasu Yamamuro[8], Masanobu Ozaki[1], Takahide Mizuno[1], Yoshifumi Saito[1], Kazuyuki Touhara[1], Noriyuki Namiki[3], Hiroshi Araki[3], Hirotomo Noda[3], Shoko Oshigami[3], Jun Kimura[9], Christian Althaus[10], Simone DelTogno[10], Kay Lingenauber[10], Hauke Hussmann[10]

1.Institute of Space and Astronautical Science, Japan Aerospace Exploration Agency, 2.CIT, 3.NAOJ, 4.MRJ, 5.PLANET, 6.FAM Science, 7.Astro-Opt, 8.OptCraft, 9.Earth-Life Science Institute, Tokyo Institute of Technology, 10.DLR

We present Optical/Structural/thermal design for the receiver part of the Ganymede Laser Altimeter (GALA) for the Jupiter Icy Moon Explorer (JUICE) mission. JUICE is a mission of ESA to be launched in 2022, and GALA is one of the payloads of JUICE. For the laser altimetry, GALA emits and receives laser pulses at about 500 km altitude above Ganymede. Wavelength, energy, and repetition frequency of the laser plus are 1064 nm, 17 mJ, and 30 Hz, respectively. Reflected beam from the Ganymede surface is received by the receiver telescope with 25 cm diameter aperture, re-focused by the BEO including a narrow band-pass filter, and then detected by the APD detector. In the international collaboration, GALA-Japan will develop the Backend Optics (BEO), the Focal Plane assembly (FPA) including an avalanche photo-diode (APD) detector, and the Analog Electronics module (AEM) in the receiver chain.
Thermal environment of GALA is unique: The Receiver telescope and some parts are cooled to intermediately cryogenic temperature by radiation to the cold surface of Ganymede and deep space while the APD detector has to be kept at 25 degree in its operation time. Many parts of GALA are warmed by self-heating. Furthermore, GALA repeats observation time of 16 hours and data downlink time of 8 (power of observation part is off) hours. So the thermal environment is dynamic.
On the other hand, GALA have to keep stability of optical performance, especially absolute agreement of the optical axis of the emitter and the receiver and to the spacecraft coordinate system. Radiation shield also has to be mandatory. Considering these conditions, we are carrying out design of optics, structure and thermal design for the BEO, FPA, and AEM. The current baseline design, the BEO is simply consisting of a collimator lens, a narrow band-pass filter, a focusing lens supported without adhesive. The material used for the structural material of both BEO and FPA must have small thermal expansion and good radiation shielding. Iterative studies of thermal analysis of whole GALA and the optical/thermal/structural design is ongoing.

Keywords: JUICE, GALA, optical/thermal/structural design

Non-destructive material identification of volatile particles using translational motions induced by magnetic field gradient

*Keiji Hisayoshi[1,2], Wakana Yamaguchi[1], Chiaki Uyeda[1]

1.Dept. of Earth and Space Science, School of Science, Osaka University, 2.Kasugaoka High School

Recently, we developed a new method of magnetization measurement method, in which translation induced by the magnetic field gradient was used, and proposed a material identification based on this method. Due to the field-induced energy, the solid particles which were released in a diffused area (in a condition that effect of gravity and viscous drag are negligible), causes translational motion by a practical field intensity of the permanent magnet. Because this motion derives from a magnetic volume force, the motion of the particle is independent to the mass. The material possesses the intrinsic susceptibility per unit mass. Therefore, the material of individual particles can be estimated by comparing the measured susceptibility with a list of published values. In the present study, we apply the above method to identify volatile solid grains of H_2O and CO_2.
The translational motion is observed by the chamber-type drop box. The system was realized by introducing small Nd-Fe-B plates. The setup for observing the motion was attached inside a rectangular volume of 35×30×20 cm of a drop box. The setup was enclosed in a vacuum chamber; the sample motion was observable from the outside of the Pyrex wall of the chamber, using a high-speed video camera that had time resolutions of 0.033 s. The pressure of the medium inside the camber was P =100 Pa. Duration of μG was about 0.5sec with residual gravity of 0.01G.
Previously, identification of particles using magnetic field was limited on materials with spontaneous magnetization. However, it's possible to expand the method to general solid particles. Provided that the motion of particle is observable, it's possible to measure the susceptibility of the sample no matter how small the particle may be. In the field of the organic chemistry and the biochemistry, the method to separate a mixture of organic molecules has been established by introducing the technique of chromatography. The proposed principle of material identification can be applied in an apparatus developed for a mission to examine the surface of the icy satellites.
Reference
[1] K. Hisayoshi, S. Kanou and C. Uyeda : Phys.:Conf. Ser., 156 (2009) 012021.
[2] C. Uyeda, K. Hisayoshi, and S. Kanou : Jpn. Phys. Soc. Jpn. 79 (2010) 064709.

Keywords: non-destruction distinction, translational motion , magnetic field gradient force, microgravity, volatile particle

Electromagnetic induction in icy moons of Jupiter - A review and its future perspective

*Hiroaki TOH[1], Taka'aki Katsura[2]

1.Data Analysis Center for Geomagnetism and Space Magnetism, Graduate School of Science, Kyoto University, 2.Department of Earth and Planetary Sciences, Graduate School of Science, Kyoto University

Internal oceans of icy moons of gas giants of our solar system are among recent hot topics in planetary sciences. Newly discovered evidence for hydrothermal vents in the liquid ocean of Enceladus (Hsu et al., 2015) is still fresh in our memory. Presence of the internal oceans is one of the necessary conditions for extra terrestrial life, although interaction of liquid water with the lithosphere of the icy moon in concern via, say, the hydrothermal activity, is also indispensable. It, therefore, worth revisiting the problem of internal oceans of Jupiter's Galilean satellites with icy surfaces at this time of coming successive Jovian probe missions such as Juno (Bagenal et al., 2014), JUICE (ESA, 2014) and so on.

The latter three of the four Galilean satellites, Io, Europa, Ganymede and Callisto, are covered with ice, while intense volcanic activity is ongoing on the Io’s surface due to the immense tidal force of Jupiter. Those volcanic ejecta become a dense source of plasmas of Io origin, which results in Io’s footprints of Jupiter’s auroras (e.g., Bonfond et al., 2013). It is noteworthy that the former three of the Galilean satellites have those footprints, while Callisto alone lacks in them implying a very thin plasma environment around that moon as it is the farthest to Jupiter without any significant source of plasmas from Callisto itself. This means that Callisto is least subject to the plasma effect in terms of electromagnetic induction.

Another feature of Callisto that is worth noting is its orbital state. While the former three revolutions are in the state of Laplace Orbital Resonance (Murray and Dermott, 1999), Callisto alone is out of it. This may cause a significant difference in tidal force which each moon feels. Tidal dissipation is one of the important factors (Chen et al., 2014) when we consider the heat source that maintains the internal oceans of the icy moons, if any.

In this study, we reanalyzed the vector magnetic field data at the time of Galileo Probe flybys around Callisto. Assuming a time-varying uniform external magnetic field (Khurana, 1997; Khurana and Schwarzl, 2005) with a direction almost parallel to the direction of Jupiter looking from Callisto, we calculated the induced dipole field generated by concentric spherical shells. As a result, a conductive shell with a similar conductivity of seawater on the Earth was found when the depth to it was constrained by an assumed phase diagram of water inside Callisto, which coincides with previous studies (Khurana et al., 1998; Zimmer et al., 2000).

However, if the internal structure of Callisto is significantly different from those of Europa and Ganymede in the sense that Callisto has experienced immature differentiation unlike rest of the two, Callisto may provide a better platform for extra terrestrial life by an increased chance for liquid water-lithosphere interaction. In this presentation, the obtained electrical structure will be further examined comparatively with that of Europa known to date. Comparison with that of Ganymede may be subject to another research because of the moon's peculiar intrinsic core field.

Keywords: Icy moons, Jupiter, Electromagnetic induction

Stability of liquid methane on Titan's surface

*Shuya Tan[1], Sho Sasaki[2]

1.Department of Earth and Planetary Science, Graduate School of Science, The University of Tokyo, 2.Department of Earth and Space science, Graduate School of Science, Osaka University

Titan has liquid methane on the surface due to surface conditions affected by the temperature profile of its thick nitrogen atmosphere. The purpose of this study is to discuss the stability of the surface environment, by estimating relationships between liquid methane on the surface and parameters which affect characteristic of the atmosphere. The typical parameters are the solar flux, the gravitational acceleration and so on.

Strictly speaking, present state of body like Titan depends on the evolution from its formation. But there are different scenarios for the formation of icy satellites, and moreover, the evolution is modified by external factors such as impacts and tidal heating. Here, we conduct parameter changes on the basis of the present Titan’s condition.

We use an analytic radiative-convective model for plate-parallel atmosphere (Robinson et al., 2012). On convective region, we consider the condensation of methane.

In Titan’s atmosphere, radiation is affected by absorption of thermal infrared by gas molecules and absorption of visible light by photolysis organic haze, which mainly exists in its stratosphere. The visible absorption by haze causes cooling the surface. We relate the mole fraction of methane to infrared absorption coefficient (Nakajima et al., 1992). The strength of visible absorption is probably changed by methane concentration in stratosphere and haze optical property and so on. In the present study, for simplicity, we hypothesize the simple cases, the strength of haze absorption is constant or expressed by simple function.

On this model, about liquid methane on the surface, the solar flux has lower limit caused by methane condensation. And if greenhouse effect is stronger than cooling by haze, the solar flux can have upper limit. Nitrogen partial pressure on the surface only affects the latter, and the gravitational acceleration affects both.

When the strength of visible absorption by haze is constant, the solar flux has the upper and lower limits regardless of nitrogen pressure on the surface and gravitational acceleration. The present solar flux matches the lower limit when nitrogen partial pressure is 1.06×10^6 Pa or the gravitational acceleration is 0.15 m/s^2 .

A study on surface roughness in thermo-physical modeling of asteroid for the estimation of thermal inertia

*Jun Takita[1], Hiroki Senshu[2], Satoshi Tanaka[3]

1.Graduate School of Science, Tokyo University, 2.Chiba Institute of Technology/PERC, 3.JAXA/ISAS

This study reports preliminary results of our study about the effect of rough surface on thermal inertia from thermal phase delay using thermo physical model (TPM). In the thermal modeling of asteroid, information on the surface topography and surface roughness is indispensable for thermophysical estimation, which is especially important to deduce thermal inertia of an asteroid. This is one of the preparations for the thermo-physical observations of asteroid Ryugu using the thermal infrared imager in Hayabusa2 mission.
For numerical approach using TPM, we produced rough surface models by deforming a spherical surface mesh. We considered the effect of surface roughness on surface temperature as a function that changes only the effective emissivity of the planetary surface, following the works of Davidsson et al. (2009) and Leyrat et al. (2011).
We fitted the surface temperatures that were generated by the rough surface models to determine whether the thermal phase delay can still be retrieved under rough surface topographies. We picked only the surface temperatures on the equatorial zone. Quadratic least-square fitting is applied to the data to deduce thermal phase delay.
We evaluated uncertainties in the estimation of the phase delay based on a series of data generated in the diurnal motion. As a result, we found that the feasibility of thermal inertia from the diurnal phase delay depended greatly on the observational geometry in terms of solar illumination over the asteroid surfaces. The thermal phase delay could be determined without being strongly affected by local topography under low solar phase angles. Considering the errors of phase shift, the uncertainty of thermal inertia will be greater than 50% if the rough scale is greater than 9.6° (RMS surface slope angle) from the case of low solar phase angle.

Keywords: asteroid, thermal inertia, surface roughness

Relationship between formation age and the degree of degradation of the lunar craters

Fumiki Muto[1], *Tomokatsu Morota[1], Junichi Haruyama[2]

1.Graduate School of Environmental Studies, Nagoya University, 2.Japan Aerospace Exploration Agency

Impacts of micro projectiles erode the lunar surface. Unraveling the time-scale for topographic degradation on the lunar surface is fundamental for understanding processes of the migration of regolith and the bombardment history and developing new dating method for the lunar surface. In this study, I performed crater morphologic analysis based on a topographic diffusion model to reveal the relationship between formation age and the degree of degradation for lunar craters and to evaluate the topographic diffusivity on the lunar surface. Digital Terrain Model (DTM) derived by Kaguya/Terrain Camera was used to investigate the crater shapes and the optical maturity parameter (OMAT), which characterizes the immaturity of lunar soils, was used as an indicator of the formation age for craters. The shapes of craters with fresh ejecta show that crater depth is affected by the local subsurface structure, while there is no difference of the slope of inner wall among fresh craters. Therefore, I evaluated the degree of degradation using the slope of inner wall. I found that there is a negative correlation between the degree of degradation and OMAT. Using the relationship the topographic diffusivity was estimated to be 13–31 m^2/Myr.

Keywords: crater, crater degradation, impact, Moon

Statistical analyses of bright ray craters on Ganymede: implications from Galileo and Voyager images

*Luyuan Xu[1], Hideaki Miyamoto[1], Naoyuki Hirata[2]

1.The University Museum, The University of Tokyo, 2.Kobe University

Ray craters are impact craters surrounded by radial rays or ejecta patterns (both bright and dark) and prominent on Ganymede, the biggest satellite of Jupiter. Bright ray craters are recognized to be the youngest features on Ganymede [1], and represent the most recent impact cratering [2]. Also, being susceptible to destruction by various processes [1-3], bright ray craters may inform on the most recent geologic processes on Ganymede.
Passey and Shoemaker [4] identified 84 bright ray craters D>30 km and obtained several preliminary results and conclusions using the image data of Voyager. However, since Voyager 1 and 2 only have sufficient resolution (better than 2 km/pixel) images limiting to the subjovian and antijovian surroundings [4, 5], the analysis of Galileo images could fill in this gap. Also, the revised global geologic map [5] and advanced cratering impact model [2] make a more accurate distribution and a more comprehensive understanding of bright ray craters of Ganymede possible.
In this study, we used the raw images of both Voyager and Galileo images (825 Voyager images and 314 Galileo images) to identify ray craters. Since the crater rays are sensitive to solar illuminations [2] and the coverage limitation of images, we only measured the ray craters at high sun conditions and in the latitudinal range 70°N-70°S [5]. Also considering the identifiable sizes of ray craters are highly dependent on spatial resolution of images, we initially examined the influence of image resolution on the density distribution of ray craters.
Ultimately, our work resulted in a revised density distribution of bright ray craters corresponding to spatial resolution, latitude, angular apex distance, and different terrain types, finding that the crater density of bright ray craters on Bright Terrain of Ganymede is at least ~4x from apex (the center of the leading hemisphere) to antapex (the center of the trailing hemisphere), and the bright rays are likely to be erased at a higher rate with increasing latitudes. Based on our results, we reconsidered the possible reasons for cratering asymmetry on Ganymede [2], and confirmed the influence of latitude-related factors, which might include thermal-driven sublimation [6] and plasma-induced sputtering [7].
References
[1] Shoemaker E. M. et al. (1982) Satellites of Jupiter: 435-520.
[2] Zahnle K. et al. (2001) Icarus, 153, 111–129.
[3] Schenk P. M. and McKinnon W. B. (1991) Icarus, 89, 318-346.
[4] Passey Q. R. and Shoemaker E. M. (1982) Satellites of Jupiter: 379-434.
[5] Patterson G. W. et al. (2010) Icarus, 207, 845-867.
[6] Squyres S. W. (1980) Icarus, 44, 502-510.
[7] Khurana K. K. (2007) Icarus, 191, 193-202.

Keywords: Ganymede, bright ray craters, Galileo images

The discrimination experiment of meteorites using LIBS for the Martian Moons Explorer mission

*Misa Horiuchi[1], Kazuo Shibasaki[1], Yuichiro Cho[1], Shingo Kameda[1], Ko Ishibashi[2], Koji Wada[2], Takashi Mikouchi[3], Tomoki Nakamura[4], Seiji Sugita[3]

1.Rikkyo University, 2.Planetary Exploration Research Center, Chiba Institute of Technology, 3.The University of Tokyo, 4.Tohoku University

Phobos and Deimos are the two satellites of Mars. It is suggested that they originated either through asteroid capture or giant impact [1]. The Japan Aerospace Exploration Agency (JAXA) is planning to launch the Martian Moons Explorer (MMX) in 2022 that aims to return samples from Phobos. It is hoped that these samples will reveal the origin of Phobos and, thereby, will constrain the theory of Solar System formation. The sampling site will be selected based on Phobos' entire reflection spectra to return optimum samples containing intrinsic materials to Phobos. However, the reflection spectra may not provide sufficient information on the composition of Phobos because of space weathering. In addition, the composition of Phobos's surface in particle scale has unknown and isn't known until the samples are returned to the Earth. Therefore, we focused on in-situ measurement of elemental composition, which isn't affected by space weathering. We proposed mounting a laser-induced breakdown spectroscopy (LIBS) on the MMX lander for measuring the elemental composition of the Phobos's surface.
We conducted LIBS experiment to evaluate the feasibility of LIBS measurement on Phobos. We investigated the capability of distinguishing carbonaceous chondrite from Martian meteorites by LIBS, which provides a clue to knowing whether the surface of Phobos is composed of asteroid-like or Martian-like materials. Our experimental system simulated an actual setup for Phobos exploration. We used a small laser with an output of about 12 mJ/pulse and a wavelength of 1534 nm. The wavelength range of the spectrometer was 195 nm to 1128 nm. The distances between the lens to converge the laser beam and the sample, and between the condensing lens of the spectrometer and the sample were both 1.5 m. The effective diameter of the light collection optical system was 20 mm. The samples were placed in a vacuum chamber. We verified the feasibility of LIBS measurement including signal-to-noise ratio under such realistic conditions. The samples were Allende (a carbonaceous chondrite), NWA1068 (a Martian meteorite), and Zagami (a Martian meteorite). The sample was irradiated 150 times on each measurement point with 10 Hz. The exposure time of the spectrometer was 1 s. We measured 16 points per a sample to obtain the bulk composition of the meteorites. The emission spectra of the major elements, Fe, Ca, Al, Mg, Si, and Ti, were detected in the average spectra of 16 measurement points. By subtracting the spectra of the Martian meteorites from that of the carbonaceous chondrite, we found that the intensity of the emission lines of Fe and Mg, which are abundant in the Allende meteorite, exhibit positive values. In contrast, the intensity of the emission lines of Al and Ca, which are abundant in the NWA1068 and the Zagami meteorites, exhibit negative values. Those results show that LIBS can distinguish between asteroid-like and Martian-like materials.
Since the MMX lander can stay on the surface of Phobos for only about 1 hour, we evaluated whether LIBS can conduct the same measurement as our experiment in such a short time. It was assumed that the focus adjustment and image acquisition takes 10 s, and moving from one measurement point to another takes 20 s. The laser irradiation frequency is 2 Hz to save the electric power consumption. Then, it takes 28 minutes to conduct the same date acquisition as our experiment (i.e., measuring 16 points with 150-times laser irradiation per point).This indicates that LIBS can obtain sufficient data within the operation time of the lander. Our results suggest that LIBS can reveal

whether Phobos is similar to asteroids or Mars.

Reference

[1] Fraeman, A. A., et al. (2012), J. Geophys. Res., 117, E00J15.

Keywords: the Martian Moons exploration project, LIBS, in-situ measurement

A new paradigm to solve "the missing link of "Moon and Earth"" is "Multi-Impact Hypothesis", it explains both Origin of the "Moon formation and the Earth's plate tectonics" and Formation of Mercury

*Akira Taneko[1]

1.SEED SCIENCE Lab.

In the scientific method to explore the origin of the previous solar system where life, including human beings occur, deductive method, and a creative subjunctive in addition to induction.It means to discover the truth in the induction method, an observation or experiment of Earth evolution.There was nothing other than the Earth observation until now as the way.Hypothesized, the hypothesis is believed as the conclusion is often the more that can explain the current situation.
Now, in the Abduction creative reasoning, is the idea of correctness is increased if be said in reverse.It is a perfect way to explore the origins and mysteries, but If you do not have thought a breakthrough hypothesis, have no sense at all.
The "Multi-Impact Hypothesis," to give the hypothesis with the following "Linking the moon and the earth of the Missing Link," a unified reasoning of (A) and (B).
(A) Differentiated protoplanetary CERRA of Mars size formed in the asteroid belt position of the solar system, by the perturbation of the most recent of Jupiter (giant mass), orbit is flattened to Jupiter near point side.
(B) Immediately before the CERRA to Jupiter collision, ruptured at a tension of Jupiter and the sun, the mantle piece collide intersects the Earth orbit.
by Abduction
(1) Moon of origin: collision mantle piece to Earth (12.4km / s, 36.5 degrees), and formed in the orbit radius 60 · Re position
*(2)Pacific Rim arc-shaped archipelago marginal origin: In the Pacific Ocean position collision at the time of moon formation, Depression marginal sea forming in all directions
*(3)By a large amount of mantle deficient moon formation collision, Van Allen belt of Brazil of core eccentricity (about 10%) was reduced.
*(4)CERRA it takes about 5-6 million years until the track flat torn in Jupiter perturbation, had already differentiated cooling.
*(5)Multiple of mantle piece collide to Eartht by peeling off the mantle , 70% of the sea surface of the earth -5km was formed by isostasy.
*(6)Origin of plate tectonics PT , minimization of the eccentric and the moment of inertia caused by the collision as the driving force.
*(7))Origin of plate boundary , Crust peeling due to the mantle piece collision and crack formation
*(8)Origin of arc-shaped archipelago and Marginal basin plate : Mantle deficit by collision and plate concave formed by isostasy
*(9)The origin of the start of subduction convex plate : When the concave plate and the convex plate each other press by the driving force , cause the convex crawl under concave.
(10)Fragments at break of CERRA is the origin of the asteroid belt. Understood in the distribution of long radius (kinetic energy)
(11)The meteorite, but differentiated stony, stony-iron and iron meteorites are mixed , it can be understood with the fragments of CERRA.
(12)There are several fragments of CERRA, large species extinction repeated happened with sequentially collision.
(13)Core and part of the mantle of CERRA , the mass is large energy such as distribution, It became

a low orbital energy Mercury with law of equipartition of energy.
(14)The fragments of CERRA that has collided to Jupiter, was the origin of the Great Red Spot.
(15) Why Pluto is a stony? Jupiter and Saturn is a gas planet! I suggested. "Swing by the Serra fragments became Pluto with Jupiter"
(16)The inclination 23.5 degrees earth's axis was achieved with collision of the high latitude! Kimberlite pipe formation to the Russian Mirny mine position, By the collision of the Drake Passage , It gave a moment that the inclination of the earth's axis is changed.
(17) the inclination of the rotation axis is also changed the direction of the driving force, it can be steep bend also the description of the Emperor seamount chain.
(Description of the sudden change in the thermal convection the drive theory seems to be impossible)

Keywords: the missing link of "Moon and Earth", Origin of the "Moon formation ", Origin of the "Platet ectonics", Abduction, Formation of Mercury, Titius Bode law

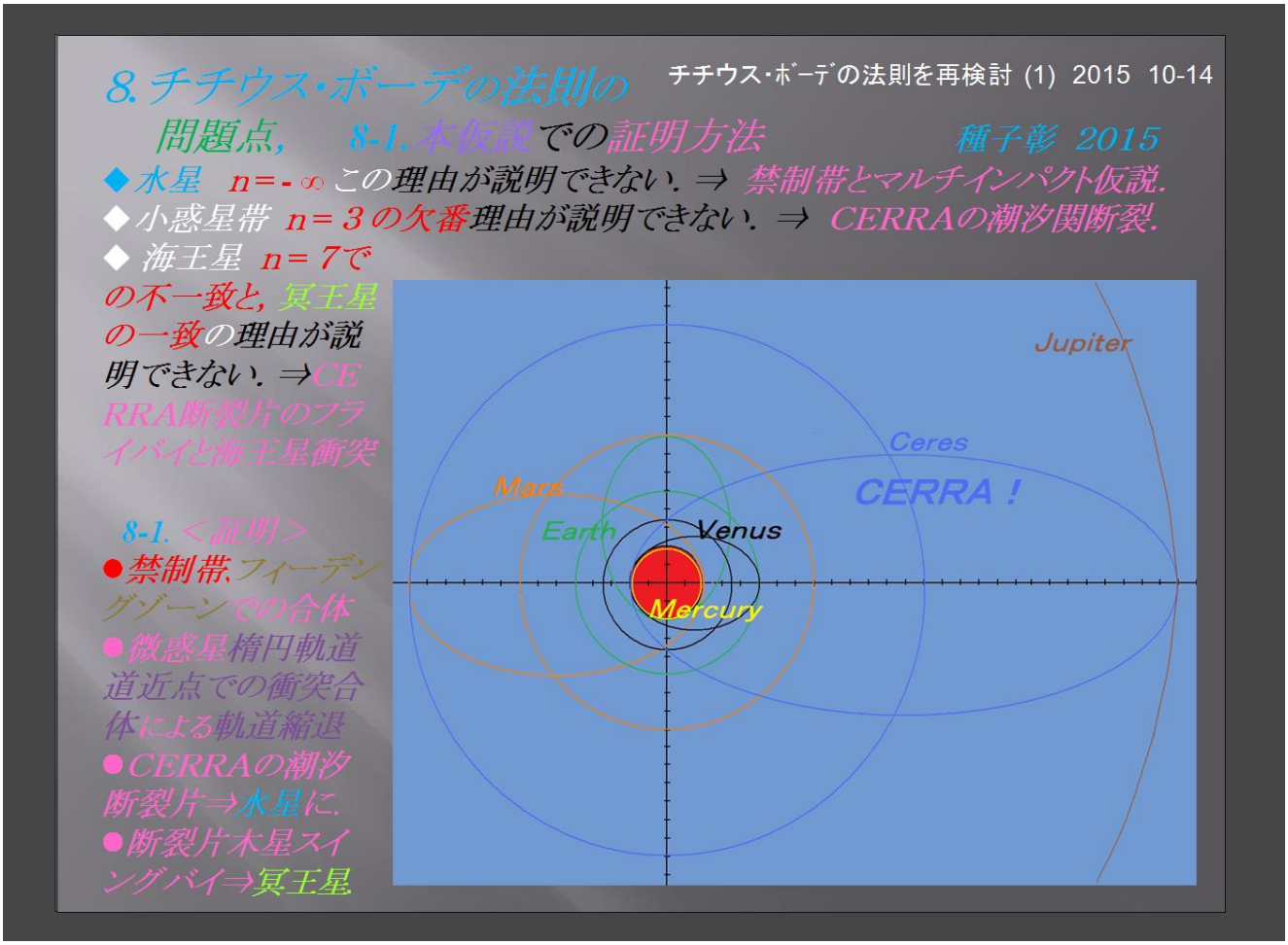

Experimental simulations on impact-induced dehydration of porous surfaces

*Jinshi Sai[1], Ryo Ogawa[2], Akiko Nakamura[2], Yusuke Seto[2], Kazunori Ogawa[2]

1.Graduate school of science, Tokyo University, 2.Graduate school of science, Kobe University

It is now generally believed that accreation of planetesimal formed planets and collision with small-bodies evolved them. Impact-induced dehydration of impactors influenced the composition of primitive planetary atmosphere and the supply of water to planets. So it is required to understand impact-induced dehydration of planetary bodies in terms of the origin of water-planets. Lots of works about small bodies to reveal the origin of the solar system and planets have been performed including sample return missions from primitive bodies. Asteroid exploration Hayabusa2 will return samples of a C-type asteroid Ryugu which possibly has hydrated minerals. Understanding impact-induced dehydration is of importance in order to discuss the influence of dehydration of the returned samples.
A lot of experimental works related with impact-induced dehydration have been performed and most of the experiments are shock recovery experiments. In this method, the samples were capsuled in sealed metal containers and impacted by projectiles indirectly. This method derived impact-induced water loss as a function of shock pressure, but didn't simulate real surface of planetary bodies very well because of the container. The relation between sample porosity and water loss has also been studied but is not fully understood. In order to discuss dehydration of asteroids due to impacts, it is necessary to reveal the relationship between dehydration efficiency and porosity in detail. In this study, we performed shock dehydration experiments without sealed containers to simulate natural impacts on the surface of planetary bodies. In addition, we used gypsum targets with different porosities and examined the relationship between porosity and shock-induced water loss. We set the sample in a cylindrical stainless container and shot a disk-shaped metal, stainless-steel or copper, projectile directly onto the surface. Targets were set inside a vacuum chamber under 0.1atm condition. We measured the velocity of projectile using a high-speed video camera. The shock pressure was calculated by impedance matching method. The post-shocked samples were recovered from the surface of the projectile. We analyzed the recovered samples by XRD and examined if dehydration occurred. After that, we measured the impact-induced water loss (wt%) by thermogravimetric analysis (TGA) and compared the results with those of XRD.
Impact-induced dehydration was observed in this study. We found that the results of XRD and TGA were consistent. We did not found any strong relationship between porosity and water loss in this work.

Keywords: impact-induced dehydration, porosity

Effect of secondary collision and target texture on three-dimensional shape distribution

*Tokiyuki Kadokawa[1], Akira Tsuchiyama[1], Tatsuhiro Michikami[2], Sunao Hasegawa[3], Tsukasa Nakano[4], Kentaro Uesugi[5]

1.Department of Earth and Planetary Sciences, Graduate School of Science, Kyoto University, 2.Kinki University, 3.ISAS/JAXA, 4.AIST, 5.JASRI/SPring-8

3D shape distributions of regolith particles returned from the asteroid Itokawa by the Hayabusa mission and the moon by the Apollo and Luna missions have been measured [1,2]. Such 3D shape distributions reflect conditions of regolith particle formation and it is important to compare with those of fragments in laboratory impact experiments to discuss impact processes on the surfaces of Itokawa and the moon.
It has been proposed based on a laboratory experiment that the 3D shapes of impact fragments have characteristic distribution; the average axial ratios of the longest, intermediate and shortest lengths of fragments, a : b : c ,is 2:√2: 1. Although the ratios of individual fragments were widely distributed [3]. As this result was obtained only in a catastrophic disruption condition, Michikami et al. [4] carried out impact experiments under wide range of impact conditions from cratering to catastrophic disruption and found that the average three axial ratios is not 2:√2: :1 when the impact energy density is low (cratering conditions). However, the size of fragments examined (>4 mm) is bigger than that of Itokawa and Luna regolith particles (20-300 um). So, we measured the axial ratios of fragments obtained from the same experiments [4] with similar size to the regolith particles, and found that (1) the size distribution depends on the fragment size, (2) the average axial ratios are almost constant around 2:√2:1 irrespective of the impact energy density and (3) the distribution cannot be distinguished from that of Itokawa particles [5]. However, effects of secondary collision and target texture have not been evaluated.
In this study, additional experiments were made in order to elucidate the effect of secondary collision and target texture. Impact experiments were carried out with a two-stage light-gas gun at JAXA. We used basalt, dunite, ordinary chondrite (L4/5) and lead glass as targets and spherical nylon (7.14 mm in diameter) or alumina (1.00 mm) as projectiles. The impact velocity ranged from 1.60 to 7.0 km/s. Two types of impact fragments (30-600 um) were examined; one is fragments collected in aerogel, which were not suffered by secondary disruption, and the other is fragments collected from the surfaces of impact absorbers. The three axial lengths were measured using X-ray microtomography in SPring-8, and their 3D shape distributions were compared with each other and with those of Itokawa and Lunar regolith particles using Kolmogolov-Smilnov test.
It was found from the experiments that the 3D shape distributions and the average axial ratios of fragments collected from aerogel cannot be distinguished from those from the impact absorber surfaces. This indicates the fragments measured by Kadokawa et al. [5] were not influenced by secondary collision or secondary collision little affected the 3D shapes. It was also found that the 3D shape distributions of the experiments using basalt targets cannot by distinguished from those using dunite and ordinary chondrite targets, while they can be clearly distinguished from those using homogeneous lead glass target, which is largely different from basalt in textures. This suggests that experiments using basalt targets can simulate impact processes on the asteroids. The present results indicate that the results of Kadokawa et al. [5] is applicable to Itokawa and Luna particles; Itokawa particles can be formed by collisional destruction, but we cannot estimate their impact conditions from the 3D shape distribution while the values of the average axial ratios of Luna particles, which is closer to unity, suggests that they were affected by gardening in the regolith layer.

[1] Tsuchiyama et al. (2011) Science, 333,1125-1128. [2] Sakurama et al. (2015) JpGU Abstract PPS23-P10. [3] Fujiwara et al. (1978) Nature, 272, 602-603. [4] Michikami et al. (2015) Icarus, 264, 316-330. [5] Kadokawa et al. (2015) JSPS Abstract O4-05.

Effects of oblique impacts on catastrophic disruption of rocky bodies simulated by quartz glass

Yuu-saku Yoshida[1], *Masahiko Arakawa[1], Minami Yasui[1], Kazunori Ogawa[1], Chisato Okamoto[1]

1.Graduate School of Science, Kobe University

Planetary collisional process is one of the most important physical processes in the solar system, especially for the planetary formation process in the solar nebulae. Because of the importance of the physical process and the implications for the origin of asteroids and other small bodies, impact disruption experiments have been conducted for several decades, and rocky materials such as basalt and glass etc. were used for these impact experiments. Then, the impact strength defined by the specific energy (Q) necessary for the catastrophic disruption was obtained for these rocky materials, and most of the impact experiments were conducted by head-on collisions, so that the impact strength was usually applicable only for the head-on collision. However, collisions among planetary bodies are well known to be not only head-on collision but also oblique collision, and actually the impact angle of 45 degrees is the most probable impact angle in the solar system. Therefore, it is necessary to study the impact strength for the oblique impact and to clarify the effect of oblique impact on the collisional disruption of rocky bodies.
In this study, we conducted the impact experiments of quartz glass at the impact angle from 90 (head-on collision) to 0 (glancing impact) degrees, and studied the effect of oblique impacts on the degree of disruption and the ejection velocity of the ejecta fragments. We used quartz glass spheres with the size of 5cm and 8cm for the target, and a polycarbonate spherical projectile with the size of 4.75mm was launched at the impact velocity from 2 to 6km/s. The oblique impact was made at 15 to 90 degrees at 4.3km/s under the vacuum condition of 20Pa. After the impact, all the impact fragments were recovered to measure each weight in order to construct the size distribution of these fragments.
We found that the largest fragment mass was almost constant at the impact angle from 90 to 60 degrees, and it suddenly decreased from 60 to 45 degrees for the 5cm target, and then gradually increased up to 15 degrees: the largest fragment mass at 45 degrees was one order of magnitude larger that obtained from the impact between 90 and 60 degrees. Although the impact strength could be strongly affected by the impact angle at the high obliquity smaller than 45 degrees, the modified specific energy (Q_c) defined by the normal component of the impact velocity on the impact surface was an appropriate parameter to scale the impact angle on the degree of the impact disruption, then the impact strength (Q^*) could be refined by using this modified specific energy, Q_c: The obtained impact strength defied by Q_c including the oblique impacts is 1110 J/kg for the quartz glass. We also found a very unique feature on the quartz glass during the disruption, that is, the severe disruption and high velocity ejecta was discovered at the antipodal region. The mass of disrupted fragments originated from the antipodal region was almost same as that was originated from the cratered region near the impact site. This might be caused by the severe concentration of the shock wave at the antipodal region and it would be reflected on the free surface with the perfectly spherical shape of the quartz glass. But, further research would be necessary to understand this unique features discovered at the antipode.

Keywords: catastrophic disruption, oblique impact, impact strength

Shock induced vitrification, defect generation, and change in cathodoluminescence of quartz: possibility as a new shock barometer

*Yu Chang[1], Masahiro KAYAMA[2], Eiichi Tajika[3], Yasuhito Sekine[1], Toshimori Sekine[4], Hirotsugu Nishido[5], Takamichi Kobayashi[6]

1.Department of Earth and Planetary Science, Graduate School of Science, The University of Tokyo, 2.Planetology, Kobe Univ., 3.Complexity Sci. & Eng., Univ. of Tokyo, 4.Earth & Planetary Sci., Hiroshima Univ., 5.Research Institute of Natural Science, Okayama Univ. of Science., 6.National Institute for Material Science (NIMS)

Impact cratering is a ubiquitous process on both terrestrial planets and small bodies in the solar system. Researches for impact craters on the Earth provide a valuable opportunity to constrain planetary-scale impact event. In particular, reconstruction of shock pressure recorded in the shock-metamorphosed minerals leads to a clue to understand a partition of the impact energy and cratering mechanism on Earth.
Quartz, which is one of the most abundant and widely distributed rock-forming mineral on the Earth's crust, has been widely used to evaluate shock pressure on the impactite. However, the conventional shock estimations based on the mineralogical features of quartz, such as PDFs, are no more than a qualitative approach, hence it is required for more detailed evaluation of shock pressure to develop new advanced method using quartz.
Recently, we found the drastic change in cathodoluminescence (CL) features of quartz due to shock metamorphism [1]. The blue emission intensity (450-460 nm) of shocked quartz increases drastically with the experimentally induced pressure and reaches up to 100 times as large as that of the starting materials. On the other hand, CL intensity around 630 nm changes less than 3 times in spite of the pressure increase. Therefore, the relationship between shock pressure and blue CL intensity could be used as a new shock barometer. The mechanism for the increase in the blue CL intensity, however, still remains unclear because of a lack of information on structural defect in shocked quartz. In this study, Raman spectroscopy and EBSD analysis were conducted for the experimentally shock-induced quartz to clarify the structural change and generation of misorientations with the pressure. Consequently, we elucidated the CL mechanism of shocked quartz by comparison with the obtained Raman and EBSD data.
Raman spectra of the shocked quartz show a weakening of the main peak at ~464 cm^{-1} with pressure increase. At 30 GPa, the new peak at ~495 cm^{-1} appears, indicating the generation of shock-densified silica glass [2]. EBSD mapping revealed that shocked quartz undergo high pressure (~20 GPa) has high-density domains with boundary misorientation dominated by 60°, suggesting the development of Dauphiné twinning. However, for the quartz undergo pressure over 30 GPa, EBSD diffraction pattern was unrecognized because of low crystallinity. Therefore, the blue CL emission is closely related to Dauphiné twin, but this phenomenon is limited to the pressure lower than 30 GPa. On the other hand, the destruction of crystal structure and generation of high-density silica glass are consistent with the continuous increase in CL intensity of blue emission with pressure increase. These facts indicate a spectral change depending on the extent of vitrification. The relationship between CL intensity and the possibility as a new shock barometer will be also discussed.
[1] Chang et al., (2015) JpGU Meeting, PPS22-19.
[2] Okuno et al., (1999) PCM, 26, 304-311.

Keywords: shock metamorphism, shocked quartz, cathodoluminescence, micro-Raman spectroscopy, EBSD

Radiation mechanism of the Chelyabinsk superbolide

*Masahisa Yanagisawa[1]

1.The University of Electro-Communications

On Feb. 15, 2013, a meteoroid with a size of about 19 m plunged into the terrestrial atmosphere at 19 km s^{-1} and burst at an altitude of about 30 km over the city of Chelyabinsk, Russia. Here we present light curves for the bolide in the red, green, and blue color bands, derived from an analysis of a video that was recorded by a dashboard camera and released on the Internet (Fig. 1). Our results demonstrate that the bolide was blue-green in color, which is inconsistent with the Planck spectrum before the meteor began to fragment. Fragmentation triggered a flare-up of the bolide and 90% of its radiation energy at optical wavelengths was released within a period of about 2 s after that. During the same period, the brightness ratios among the three bands became consistent with 4000 K blackbody radiation. Based on the peak luminosity, a surface area of several square kilometers would be required for a 4000 K blackbody. It is considered that the radiation source of the bolide was an elongated cloud of vapor and debris produced through severe fragmentation of the meteor.

Reference: M. Yanagisawa, Radiative characteristics of the Chelyabinsk superbolide, Planetary and Space Science., 118C, 79-89, 2015.

Figure 1. (a) Bandpass photometric intensities for the Chelyabinsk bolide plotted as functions of the bolide altitude. The thick, thin, and dotted lines respectively show the intensities in the R, G, and B bands. The black triangles indicate the altitudes at which meteor fragmentation occurred, with the upper two triangles corresponding to severe fragmentation events. (b) Color temperatures for the bolide as functions of altitude. The thick, thin, and dotted lines show the temperatures based on the R/G, G/B, and R/B intensity ratios, respectively. The error is expected to be about ± 400 K.

Keywords: Chelyabinsk, bolide, fireball, meteor, meteoroid, hazard

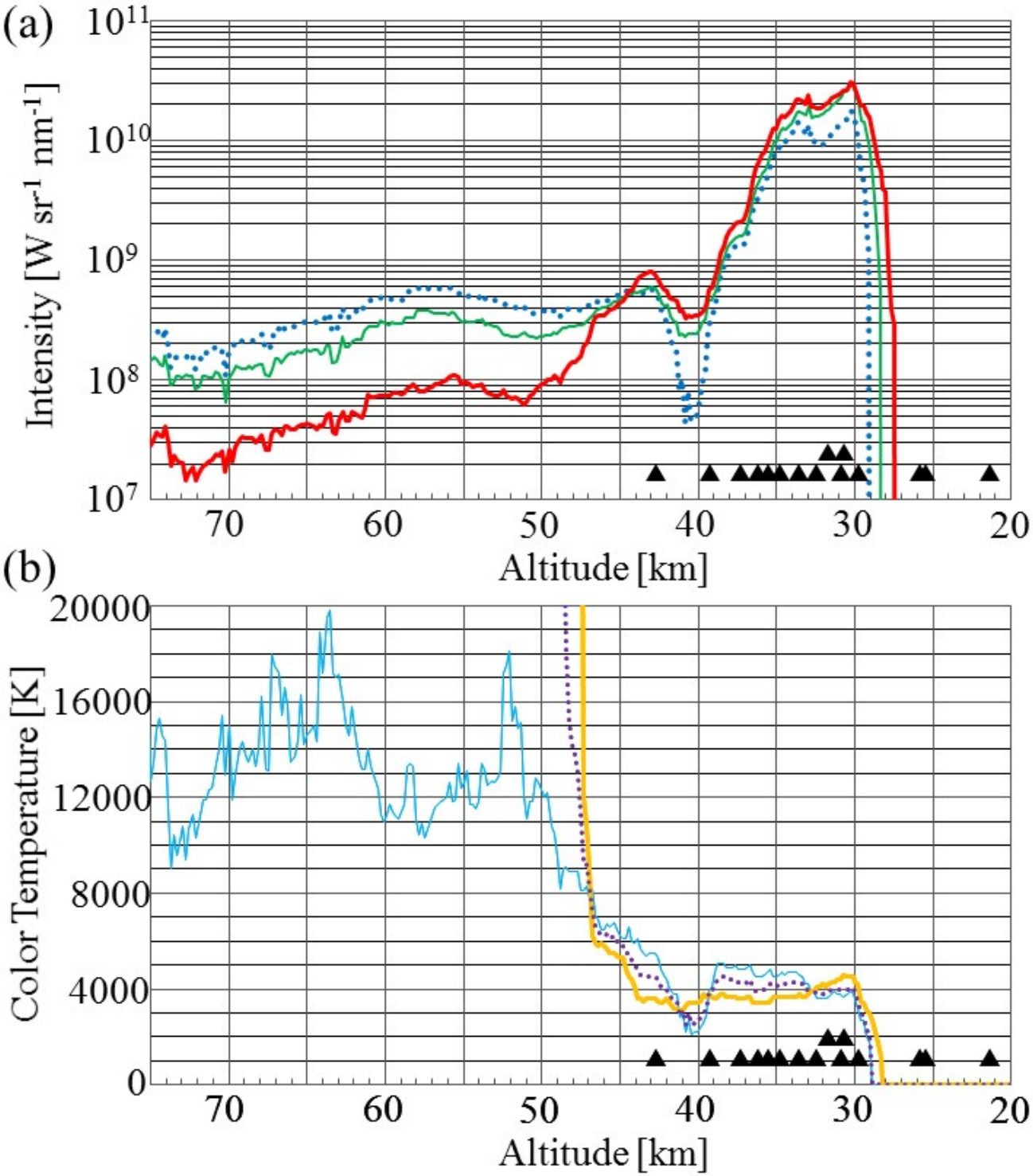

Capture of small bodies by a giant planet

*Arika Higuchi[1], Shigeru Ida[2]

1.Tokyo Institute of Technology, 2.Earth-Life Science Institute, Tokyo Institute of Technology

We have investigated the dependence of the prograde/retrograde temporary capture of asteroids by a planet on their original heliocentric semimajor axes through analytical arguments and numerical orbital integrations in order to discuss the origins of irregular satellites of giant planets. We found that capture is mostly retrograde for the asteroids near the planetary orbit and is prograde for those from further orbits. An analytical investigation reveals the intrinsic dynamics of these dependences and gives boundary semimajor axes for the change in prograde/retrograde capture. The numerical calculations support the idea of deriving the analytical formulae and confirm their dependence. Our numerical results show that the capture probability is much higher for bodies from the inner region than for outer ones. These results imply that retrograde irregular satellites of Jupiter are most likely to be captured bodies from the nearby orbits of Jupiter that may have the same origin as Trojan asteroids, while prograde irregular satellites originate from far inner regions such as the main-belt asteroid region.

Keywords: irregular satellites, small bodies

Capture of planetesimals by gas drag

*Ryo Suetsugu[1], Keiji Ohtsuki[1]

1.Graduate School of Science, Kobe University

Regular satellites of the giant planets in the Solar system are moving on nearly circular and coplanar orbits, thus they are thought to be formed in circumplanetary gas disks. Solid materials in the circumplanetary disk that formed satellites are supplied from the protoplanetary disk. Canup & Wards (2002) assumed that the major building blocks of regular satellites are meter-sized or smaller bodies that are brought to the disk with the gas inflow from the protoplanetary disk. On the other hand, supply of solid bodies to circumplanetary disks has been recently studied in detail using orbital integration (Fujita et al. 2013, Tanigawa et al. 2014). These works showed that bodies that are sufficiently large to be decoupled from the gas flow can contribute to the formation of regular satellites. Influence of captured solid bodies on satellite system formation would vary depending on the timing of capture. When planetesimals are captured by gas drag from the circumplanetary disk in the midst of accretion of regular satellites, part of captured planetesimals would contribute to the growth of satellites, while the rest spirals into the central planet. However, the circumplanetary disk dissipates at some point due to either gap formation in the protoplanetary disk or global dispersal of the protoplanetary disk. Planetesimals captured by such a waning circumplanetary gas disk would survive in the disk for a long period of time, and may become irregular satellites after the dispersal of the disk.
However, capture of planetesimals by weak gas drag from waning circumplanetary disks has not been examined in detail. Cuk & Burns (2004) examined capture of irregular satellites by waning disks in the late stage of planet formation, and discussed the origin of a cluster of prograde irregular satellites of Jupiter. Assuming that the cluster members are collisional fragments derived from a single body, they integrated orbits of the cluster progenitor backward in time until it escaped from the planet's Hill sphere, taking account of weak gas drag from the circumjovian disk. They found that some planetesimals captured into prograde orbits about Jupiter likely experienced a period of temporary capture before permanent capture. However, Cuk & Burns (2004) mainly focused on the capture of prograde irregular satellites and did not examine capture and orbital evolution of retrograde irregular satellites.
In the present work, we examine capture of planetesimals in waning circumplanetary gas disks using three-body orbital integration. In addition to the process of capture, we also examine subsequent orbital evolution of captured planetesimals. We find that some of captured planetesimals can survive in the circumplanetary disk for a long period of time under such weak gas drag. Captured planetesimals have semi-major axes smaller than about one third of the planet's Hill radius. Distributions of their eccentricities and inclinations after disk dispersal depend on the strength of gas drag and the timescale of disk dispersal, and initially strong gas drag and quick disk dispersal facilitates capture and survival of planetesimals. However, in such a case, final orbital eccentricities and inclinations of captured bodies remain rather large. Although our results suggest that some of the present irregular satellites of gas giant planets with small semi-major axes would have been captured by gas drag, other mechanisms are required to fully explain their current orbital characteristics.
Also, gas drag capture was proposed as the origin of the Martian satellites, but has not been examined in detail. Thus, we also examine capture of planetesimals by gas drag form a spherically symmetric atmosphere.

Keywords: Planet, Satellite, Planetesimal

Possibility of Planetesimal Formation in Disk Formation Stage

*Kenji Homma[1], Taishi Nakamoto[1]

1.Department of Earth and Planetary Sciences, Tokyo Institute of Technology

Planets are formed from planetesimals, so it is important to reveal planetesimal formation processes to elucidate the origin of our solar system and extrasolar planetary systems. It is thought that planetesimals are formed from micrometer-sized grains called "dust", which are present in the protoplanetary disk. They collide each other, coagulate, and grow to form planetesimals. However, there are some obstacles in this process. One of the most serious obstacles is the "radial drift barrier": macroscopic aggregates experience the head wind from the disk gas, lose their angular momentum with respect to the central star, and drift toward the star.
On the other hand, it is suggested that highly porous dust aggregates break through the radial drift barrier. In the minimum mass solar nebula model, highly porous icy dust aggregates can grow to planetesimal-size objects inside 10 AU (Okuzumi et al. 2012), though the model did not consider the evolution of the gas disk. It is necessary to take the gas disk evolution into account for the dust coagulation, because when the dust growth starts depends on physical conditions of the disk. In this study, we consider that both the evolution of the gas disk and the growth of the dust aggregates take place simultaneously. We simulate the viscous evolution of the gas disk starting from the molecular cloud core collapse and simulate the size evolution of icy dust aggregates with their porosities. As a result, we found that when the initial angular velocity of the molecular cloud core is large and the viscosity of the gas disk is small, dust aggregates can grow to planetesimal-size objects via direct collisional growth. In those cases, a large amount of icy dust particles can be supplied outside the snowline before icy aggregates start to drift toward the central star. Our results also suggest that icy planetesimals may be formed within a few hundred thousand years after starting the molecular cloud core collapse.

Orbital evolution of planetesimals in circumplanetary gas disks

*Hiroshi Kawamura[1], Keiji Ohtsuki[1], Ryo Suetsugu[1]

1.Kobe University

Growing giant planets have circumplanetary disks around them in the late stage of their formation if their mass is sufficiently large. Regular satellites of the giant planets are orbiting in the prograde direction in approximately circular and co-planar orbits, thus they are thought to be formed in the circumplanetary disks. Clarification of the formation processes of regular satellites, which account for most of the total mass of the satellite system is essentially important. Shimizu & Ohtsuki (in preparation) investigated orbital evolution of planetesimals in circumplanetary gas disks by three body orbital integration neglecting gravitational interaction between planetesimals. Interaction between planetesimals may become important when they are large enough and are captured in mean motion resonances of the protosatelite. In the present work, we examine orbital evolution of planetesimals in circumplanetary gas disks by N-body simulation, taking account of their gravitational interaction.

Keywords: Satellite formation

Streaming instability in the dust layer of a protoplanetary disk

*ryo hasegawa[1]

1.graduate school of science the university of tokyo

Two conflicting models are proposed to explain the process that dust grains grow to become planetesimals in the protoplanetary disk.One of them is that km-sized planetesimals are formed by the self-gravitational instability in a dust layer due to dust precipitation to the midplane. The gravitational instability occurs when the dust density exceeds a critical value. However, dust layer is believed to be in turbulent state, the layer would be dissipated.The streaming instability (Johansen & Youdin 2007) due to velocity shear between gas and dusts in the radial direction in the dust settling layer is a candidate to overcome this issue since the dust density increases locally even in the turbulent state.
We study the streaming instability by using hybrid simulations, where gas and dusts are treated as fluid and particles, respectively, and the dust-to-gas mass ratio is set to be ~1.
We show the time history of the maximum dust density due to the instability in the dust layer.

Sintering of icy dust aggregates by vertical diffusion in a protoplanetary disk

*Kiriko Kodama[1], Sin-iti Sirono[1]

1.Graduate School of Environmental Studies, Nagoya University

A protoplanetary disk consists of gas and dust grains. Coagulation of dust grains is the first step of planetary formation. Therefore, it is important to know whether dust grains can grow or not. There are two types of dust grains. One is made of ice and the other of rock. In this study, we focus on icy dust grains. Icy dust aggregates are sintered when they are heated. Sintering is the material transfer phenomenon to decrease total surface area. When an icy dust aggregate is sintered, its neck connecting dust grains grows. Because collision between sintered dust aggregates results in bouncing, they can not grow. Therefore, sintering greatly affects planetary formation. In a protoplanetary disk, the heat source is visible light irradiation from the central star. Because the dust grains around at the equatorial plane blocks the irradiation, only dust grains around the surface of a protoplaneary disk can be heated. Therefore, if turbulence transports an icy dust aggregate to the surface having high temperature, sintering can proceed.
Using temperature profile at the midplane, timescale required for sintering was estimated by Sirono (2011, ApJ, 735, 131). However, this study did not take account of the vertical diffusion of icy dust aggregates. In this study, we calculate the vertical motion of dust aggregates to clarify the sintering timescale by vertical diffusion.
The vertical motion of dust aggregates is diffusion by turbulence and sedimentation by gravity of the central star. We calculated the positions of aggregates as a function of time. Because sintering strongly depends on temperature (Sirono, 2011, ApJ, 735, 131), sintering of icy dust aggregates can be assumed to quickly proceed at certain height from the midplane. By numerical simulation we calculated the ratio of sintered dust aggregates that experienced high temperature to total number of aggregates. From this ratio, the sintering timescale is determined.
Distribution of dust aggregates reaches a steady state after the sedimentation timescale. In the steady state condition, each aggregate moves up and down in a vertical direction of a protoplanetary disk, icy dust aggregates are sintered if they exceed the altitude of high temperature. The fraction of sintered dust aggregates increases with time. The result can be well fitted by 1-exp(-t/b), where t is time and b is the sintering timescale. It is found that the sintering timescale gets shorter as the altitude of high temperature decreases. The sintering timescale is determined by the diffusion timescale that depend solely on the strength of turbulence irrespective of aggregate size. The altitude of high temperature depends on size of aggregates. As dust aggregates grow, the altitude goes down. Therefore, if they sufficiently grow, sintering by vertical diffusion of turbulence can proceed. It is possible that sintering by vertical diffusion hinders the growth of the aggregates.

Keywords: protoplanetary disk, dust aggregates, sintering, turbulence, diffusion

Water Delivery to Terrestrial Planets by Pebble Accretion

*Takeru Yamamura[1], Shigeru Ida[1]

1.Department of Earth and Planetary Sciences,Graduate School of Science and Engineering,Tokyo Institute of Technology

The Earth would contain water of 0.023wt%-1wt% on the surface(ocean) and in the interior. It is observationally suggested that early Mars and early Venus had water. In particular, the water fraction of the early Mars may be comparable to that of the current Earth. Based on this information, we have investigated the water fraction of the Earth, Mars, Venus, and Mercury delivered by pebble accretion which is actively discussed today, numerically calculating the growth and inward migration of icy pebbles.
It is suggested that the snow line once migrated down to ~0.7AU. Then, the terrestrial embryo gained water components from capturing migrating icy pebbles from outer parts of the protoplanetary disk. Because icy components have been subtracted in the outer disk, the gas in the terrestrial planet region should have been 'dry '.
Using this model, Sato et al. (2016) calculated the amount of water delivered to the Earth by icy pebble accretion and showed that a relatively small disk, strong turbulence, late passage of the snow line at 1AU are required to be consistent with the inferred water content of the current Earth. We have generalized their simulation to a system of multiple planets (Earth, Mars, Venus and Mercury). While we used the same model of migration and formation of dust grains as Sato et al. (2016), we included decrease in pebble mass flux due to accretion by each planet. We found that the final water fraction of individual planets is directly determined by total amount of solid materials remaining in the disk. As long as the snow line passage timing at the individual planetary orbits is the same for all the planets, the final water fraction of individual planets should be similar to one another, while the amount of the water fraction depends on disk size, strength of turbulence, the timing of the snow line passage.

Keywords: pebble, water, planet

Simulation of the early Martian climate with denser CO_2 atmosphere using a general circulation model

*Arihiro Kamada[1], Takeshi Kuroda[1], Yasumasa Kasaba[1], Naoki Terada[1]

1.Graduate School of Science, Tohoku University

The traces due to obvious liquid flow, which are thought to be made ~3.8 billion years ago, have been found on the Martian surface. They are believed to be made by the flow of liquid H_2O, and the environment of the ancient Mars is thought to be warmer and wetter than today. Several modeling studies have been performed for the investigation of the possible warming processes, but a study using a Martian general circulation model (MGCM) assuming the pure CO_2 atmosphere and the solar radiation corresponding to the time (~75% of today) [Forget et al., 2013] could not reproduce the surface temperature of higher than he melting point of H_2O, ~250 K in maximum, with the surface pressure of between 0.1 and 7 bars.
We are starting to reproduce the ancient Martian environment, in which the liquid flow existed on surface, using the DRAMATIC MGCM [e.g., Kuroda et al., 2005]. As a first step, we simulated the possible climate on early Mars with the pure CO_2 atmosphere and the global average of surface pressure of between 0.1 and 5.1 bars. In our simulations, the intensity of solar radiation is set to be 75% as large as today, assuming the ancient (~3.8 billion years ago) Mars, as well as Forget et al. [2013]. The same obliquity and eccentricity as today and very weak radiative effects of dust (opacity of 0.01) are adopted. Note that our model does not consider the infrared radiative effects of CO_2 ice clouds as implemented in Forget et al. [2013].
In the results of the simulations with the mean surface pressure of lower than 1 bar, the global mean skin temperature is almost constant to be ~192K, which corresponds to the radiative equilibrium temperature. It means that CO_2 infrared radiation in the 15 micro meter band does not work well under such a low temperature. In the simulations with the surface pressure of above 1 bar, global mean skin temperature increases with pressure, along with the CO_2 sublimation temperature. The regions with the surface temperature of near the CO_2 sublimation point (200-210K) spread globally, and it is considered that the emission of latent heat in the condensation processes stabilizes the temperature. However, our simulations show lower mean surface temperature than Forget et al. [2013], maximum for ~30 K with the mean surface pressure of 2-3 bars. The distance of temperature between the models becomes smaller with higher surface pressure, and become almost zero with 5 bars. One of the possible reasons is the radiative cooling of CO_2 ice clouds. In our simulation, column density of CO_2 ice clouds increases with the mean surface pressure of up to ~3 bars, so the absorption of long-wave radiation by the CO_2 ice clouds would possibly be critical. The other is the setting of albedo in the models. Between Forget et al. [2013] and our GCM the albedo of CO_2 ice sheet is different (0.5 and 0.65 correspondingly), which results in the lower surface temperature in our model with the mean surface pressure of 2-3 bars in which the area of CO_2 ice cloud spreads.

Keywords: Mars, Paleoclimate, General circulation model

Erosion and Replenishment of Atmosphere and Ocean on Earth during Heavy Bombardment

*Yui Kozasa[1], Hidenori Genda[2], Hiroyuki Kurokawa[2], Shigeru Ida[1,2]

1.Department of Earth and Planetary Sciences, Tokyo Institute of Technology, 2.Earth-Life Science Institute, Tokyo Institute of Technology

After the Earth's formation, Earth experienced a lot of collisions of small objects such as asteroids and comets. These impacts, the so-called heavy bombardment, should have a great influence on the Earth's atmosphere. For example, the atmosphere can be eroded by the impact and also can be replenished by the volatile in the asteroid bodies. At the same time, Earth's ocean might exist in the early stage (Wilde et al., 2001). Therefore the ocean would also experience the erosion and replenishment by these impacts. The purpose of this work is to investigate the effects of these impacts on atmosphere and ocean throughout this heavy bombardment event.
There are several previous papers on atmospheric erosion caused by just one impact (Svetsov 2000, 2007; Shuvalov 2009, 2014). In these papers, the eroded atmosphere mass by a single impact was analytically and/or numerically investigated, and its dependence to impact parameters (e.g. impactor diameter, impact velocity, atmosphere pressure,) is formulated as the equations with several parameter sets. For a long-term evolution, de Niem et al. (2012) focused on the atmosphere erosion and replenishment during LHB (late heavy bombardment), which is thought to happen during 3.8 Ga. During LHB, the total impactor mass is less than 0.01% of Earth mass. By Monte Carlo approach, de Niem et al. (2012) found that the atmospheric pressure strongly increases both in Earth and Mars during LHB.
In our study, we also use a Monte Carlo calculation of atmosphere and ocean simultaneously. To consider the whole term of heavy bombardment, we computed until the total impactor mass reaches 1% of the Earth mass. We also used several atmospheric erosion models to study how the mass change behavior depends on the model. To regard the ocean mass evolution, the erosion mass of ocean is taken from the target loss mass in Svetsov (2009), which was calculated simultaneously with the atmospheric erosion. We applied the water density as the target density. For Monte Carlo calculation, we used the current size distribution of the Main belt asteroids. Impact velocity distribution is taken from a numerical model, and we used three parameters for the volatile and water content of asteroids.
As a result, the atmosphere is extensively eroded in the model of Svetsov (2000, 2007), and the atmospheric pressure converges to a certain value, which depends on the concentration of volatile amount in impactors, regardless of the pre-existing atmospheric pressure. However, the erosion of the atmosphere is minor in the model of Shuvalov (2014). The behavior of the atmospheric mass strongly depends on the erosion models used in the computation. The ocean erosion did not depend on the atmosphere in spite of the impact energy dependency to atmosphere pressure in Svetsov (2009). The erosion of the ocean is moderate than that of atmosphere. Therefore, the final ocean depth depend on the pre-existing ocean mass and water content of the impactor.
From the results of Svetsov (2000, 2007) model, the combination of extensive erosion of atmosphere and moderate erosion of ocean would explain the difference of H/C ratio between carbonaceous chondrites and the Earth's hydrosphere or bulk silicate Earth (Hirschmann & Dasgupta 2009). Also, the erosion of pre-existing atmosphere is considerable. It depends on the parameter, but the remaining ratio would be only 0.0001~10%. For this, the heavy bombardment can erode massive H-He protoatmsophere, even if the Earth got the surrounding nebular gas (Ikoma & Genda 2006). The erosion of pre-existing ocean might explain the problem that the Earth is depleted in halogen elements such as Cl, Br, and I (Sharp & Draper 2013), by thinking the elements being dissolved into

pre-existing ocean. However, in this study the ocean erosion was not effective. The erosion of pre-existing ocean is estimated about 20%, and it is not enough to explain the whole depletion of Halogen.

Keywords: heavy bombardment, atmospheric erosion, oceanic erosion

The evolutionary climatic track of the hypothetical Earth with different conditions of central star and semi-major axis

*Shintaro Kadoya[1], Eiichi Tajika[2]

1.Department of Earth and Planetary Science, The University of Tokyo, 2.Department of Complexity Science and Engineering, The University of Tokyo

The climate of the Earth is affected strongly by the insolation from the Sun and also by the amount of greenhouse gasses, especially CO_2, in the atmosphere. The former depends on the mass and age of the central star, and the semi-major axis of the planet, while the latter depends on the degassing rate of CO_2, which, in turn, depends on the thermal evolution of the planetary interiors. Thus, the climate of the Earth may be controlled both by the evolution of the planetary interior and the evolution of the host star. It is however unknown how the climate of planet could evolve if the central star and semi-major axes are different from those of the Earth today. In this study, we examine the climatic evolution of the Earth with different conditions of host stars and orbital semi-major axes.
We use a one-dimensional energy balance model coupled with a carbon cycle model to estimate the climate, a parameterized convection model coupled with a mantle degassing model to estimate the evolution of the CO_2 degassing rate, and a standard evolution model of the Sun with a relationship between mass and lifetime of main sequence stars to estimate the evolution of luminosity of the central star.
We found that, while the climate of the Earth orbiting at the inner region of the habitable zone (HZ) becomes hot owing to the increase in the luminosity of the central star, the climate of the Earth orbiting at the outer region of the HZ becomes cold because the CO_2 degassing rate of the Earth decreases with time. In particular, the Earth orbiting at the outer region of the HZ becomes the snowball climate mode after 3 Gyr, irrespective of the mass of the central star. This timescale depends mainly on the planetary parameters, such as the land fraction and land distribution. Thus, the lifetime of the habitability of the planets orbiting at the outer region of HZ is controlled largely by the evolution of the planetary interiors rather than the stellar evolution. This is essentially because the greenhouse effect of CO_2 is necessary for the planets orbiting even in the HZ to have a warm and wet climate.

Keywords: Carbonate-silicate geochemical cycle

